JACS
JOURNAL OF THE AMERICAN CHEMICAL SOCIETY

Subscriber access provided by Fudan University

Article

Mechanistic Study of an Improved Ni Precatalyst for Suzuki-Miyaura Reactions of Aryl Sulfamates: Understanding the Role of Ni(I) Species

Megan Mohadjer Beromi, Ainara Nova, David Balcells, Ann M. Brasacchio, Gary W. Brudvig, Louise M Guard, Nilay Hazari, and David J. Vinyard

J. Am. Chem. Soc., **Just Accepted Manuscript** • DOI: 10.1021/jacs.6b11412 • Publication Date (Web): 23 Dec 2016

Downloaded from http://pubs.acs.org on December 25, 2016

Just Accepted

"Just Accepted" manuscripts have been peer-reviewed and accepted for publication. They are posted online prior to technical editing, formatting for publication and author proofing. The American Chemical Society provides "Just Accepted" as a free service to the research community to expedite the dissemination of scientific material as soon as possible after acceptance. "Just Accepted" manuscripts appear in full in PDF format accompanied by an HTML abstract. "Just Accepted" manuscripts have been fully peer reviewed, but should not be considered the official version of record. They are accessible to all readers and citable by the Digital Object Identifier (DOI®). "Just Accepted" is an optional service offered to authors. Therefore, the "Just Accepted" Web site may not include all articles that will be published in the journal. After a manuscript is technically edited and formatted, it will be removed from the "Just Accepted" Web site and published as an ASAP article. Note that technical editing may introduce minor changes to the manuscript text and/or graphics which could affect content, and all legal disclaimers and ethical guidelines that apply to the journal pertain. ACS cannot be held responsible for errors or consequences arising from the use of information contained in these "Just Accepted" manuscripts.

ACS Publications

Journal of the American Chemical Society is published by the American Chemical Society. 1155 Sixteenth Street N.W., Washington, DC 20036
Published by American Chemical Society. Copyright © American Chemical Society. However, no copyright claim is made to original U.S. Government works, or works produced by employees of any Commonwealth realm Crown government in the course of their duties.

Mechanistic Study of an Improved Ni Precatalyst for Suzuki-Miyaura Reactions of Aryl Sulfamates: Understanding the Role of Ni(I) Species

Megan Mohadjer Beromi,[a] Ainara Nova,[b] David Balcells,[b,*] Ann M. Brasacchio,[a] Gary W. Brudvig,[a] Louise M. Guard,[a] Nilay Hazari [a,*] and David J. Vinyard[a]

[a]The Department of Chemistry, Yale University, P. O. Box 208107, New Haven, Connecticut, 06520, USA; [b]Centre for Theoretical and Computational Chemistry (CTCC), Department of Chemistry, University of Oslo, P. O. Box 1033, Blindern, 0315 Oslo, Norway. E-mail: david.balcells@kjemi.uio.no, nilay.hazari@yale.edu

Abstract

Nickel precatalysts are potentially a more sustainable alternative to traditional palladium precatalysts for the Suzuki-Miyaura coupling reaction. Currently, there is significant interest in Suzuki-Miyaura coupling reactions involving readily accessible phenolic derivatives such as aryl sulfamates, as the sulfamate moiety can act as a directing group for the prefunctionalization of the aromatic backbone of the electrophile prior to cross-coupling. By evaluating complexes in the Ni(0), (I), and (II) oxidation states we report a precatalyst, (dppf)Ni(*o*-tolyl)(Cl) (dppf = 1,1'-bis(diphenylphosphino)ferrocene), for Suzuki-Miyaura coupling reactions involving aryl sulfamates and boronic acids, which operates at significantly lower catalyst loading and at milder reaction conditions than other reported systems. In some cases it can even function at room temperature. Mechanistic studies on precatalyst activation and the speciation of nickel during catalysis reveal that Ni(I) species are formed in the catalytic reaction via two different pathways: (i) the precatalyst (dppf)Ni(*o*-tolyl)(Cl) undergoes comproportionation with the active Ni(0) species; and (ii) the catalytic intermediate (dppf)Ni(Ar)(sulfamate) (Ar = aryl) undergoes comproportionation with the active Ni(0) species. In both cases the formation of Ni(I) is detrimental to catalysis, which is proposed to proceed via a Ni(0)/Ni(II) cycle. DFT calculations are used to support experimental observations and provide insight about the elementary steps involved in reactions directly on the catalytic cycle, as well as off-cycle processes. Our mechanistic investigation provides guidelines for designing even more active nickel catalysts.

Introduction

The Suzuki-Miyaura cross-coupling (SMC) reaction is regarded as one of the most versatile and powerful methods to construct C-C bonds.[1] While palladium based catalysts have traditionally been employed for SMC reactions,[2] recent efforts have focused on the development of nickel-catalyzed methods as cost effective and sustainable alternatives.[3] Additionally, nickel catalysts exhibit unique chemical reactivity as they can often couple electrophiles that are unreactive in SMC reactions using palladium systems such as aryl nitriles,[4] aryl trimethylammonium salts,[5] *N*-acyliminium and quinolinium ions,[6] aryl fluorides[7] and sp^3-based electrophiles.[8] In particular, phenol-derived substrates, which are robust and easy to synthesize from ubiquitous phenols, are an interesting class of electrophile where nickel catalysts provide superior activity compared to palladium systems.[3a,9] Substrates containing aryl carbamates and sulfamates are especially attractive,[10] as these moieties can act as directing groups for the prefunctionalization of the aromatic backbone of the electrophile prior to cross-coupling.[11] This concept has been elegantly utilized by Garg *et al.* in the synthesis of the anti-inflammatory drug flurbiprofen via a nickel-catalyzed SMC reaction.[10c] Unfortunately, the current methodology for nickel-catalyzed SMC reactions of aryl carbamates and sulfamates is limited by the use of high catalyst loadings and harsh reaction conditions.[10] In fact, the only SMC reactions involving aryl sulfamates that occur at room temperature use neopentylglycolboronates, which are not commercially available, instead of boronic acids, and require catalyst loadings ranging from 5-10 mol%.[10d,10g,10j,10l]

The rational design of improved catalytic systems for the coupling of aryl sulfamates is difficult due to the paucity of mechanistic information about precatalyst activation, the nature of the active species during catalysis and the catalyst resting state.[10c] In fact, in general, there is considerably less knowledge about these important aspects of catalysis for nickel based cross-coupling reactions compared to palladium systems.[2,3c,12] Several different catalytic cycles have been proposed for nickel-catalyzed cross-coupling reactions including: (i) a traditional Ni(0)/(II) cycle in which oxidative addition precedes transmetallation and reductive elimination,[3c,10c] (ii) a Ni(I)/(III) cycle with steps analogous to the traditional (0)/(II) cycle,[13] or (iii) radical pathways which access Ni(0)/(I)/(II)/(III) species, with not all necessarily being catalytically active.[14]

Recently, we reported preliminary studies into the speciation of 1,1'-bis(diphenylphosphino)ferrocene (dppf) supported nickel catalysts during SMC reactions using aryl chlorides as substrates.[15] Notably, we demonstrated that a catalytically active Ni(I) species

ACS Paragon Plus Environment

forms during the reaction regardless of the starting oxidation state of the nickel precatalyst and is the predominant species at the conclusion of the reaction (Figure 1). However, although we proposed that the Ni(I) complex forms from comproportionation between Ni(0) and Ni(II) species, which are present in the reaction mixture, the elementary steps involved in the formation of Ni(I) complexes were not elucidated. Furthermore, the specific role of the catalytically active Ni(I) complex in the reaction was not clarified; we were unable to conclude whether it was an off-cycle species or a species directly on the catalytic cycle. As a result it was still unclear if Ni(I) formation should be promoted or inhibited to increase catalytic activity.

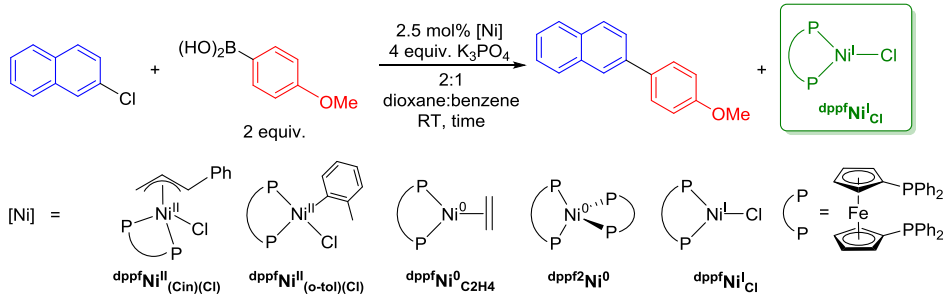

	$^{dppf}Ni^{II}_{(Cin)(Cl)}$	$^{dppf}Ni^{II}_{(o\text{-}tol)(Cl)}$	$^{dppf}Ni^{0}_{C2H4}$	$^{dppf2}Ni^{0}$	$^{dppf}Ni^{I}_{Cl}$
% yield (time)	**>99** (8 hr)	**>99** (4 hr)	**>99** (12 hr)	**>99** (4 hr)	**>99** (12 hr)
% [Ni] in the form of $^{dppf}Ni^{I}_{Cl}$ (time)	**26** (8 hr)	**44** (4 hr)	**61** (12 hr)	**22** (4 hr)	**94** (12 hr)

Figure 1. Precatalysts in the Ni(0), Ni(I) and Ni(II) oxidation state are all catalytically active for the SMC reaction with aryl chlorides. All precatalysts form a significant amount of a catalytically active Ni(I) species during the reaction.[15]

Here, we present a comprehensive study into nickel-catalyzed SMC reactions with aryl sulfamate substrates. From a synthetic perspective, by evaluating complexes in the Ni(0), (I), and (II) oxidation states, we report a precatalyst that operates at a lower catalyst loading and at milder reaction conditions than other reported systems for SMC reactions involving sulfamates.[10c,10a] *In some cases, it can even function at room temperature with boronic acid coupling partners*. From a mechanistic perspective, we provide strong evidence that the formation of Ni(I) complexes, which occurs during catalysis using our optimized system, is detrimental as it siphons catalytically active compounds out of the cycle. *It is proposed that the active species in catalysis are Ni(0)/(II) compounds and, based in part on DFT calculations, we present a detailed pathway for the formation of Ni(I) complexes via comproportionation of Ni(0) and Ni(II) species*. Our results provide guidelines on how to design improved catalysts for SMC reactions involving aryl sulfamates and related electrophiles and provide information that could be relevant to improving other types of nickel-catalyzed cross-coupling reactions including Kumada, Negishi, Hiyama, and Buchwald-Hartwig reactions,[3a-e] which may involve similar active species.

Results and Discussion

Preliminary Catalyst Screening

Previous examples of nickel-catalyzed SMC reactions of aryl sulfamate substrates and boronic acids have predominantly utilized the simple coordination complex $^{PCy}\mathbf{Ni}^{II}_{Cl2}$ as the precatalyst.[10a,10c] In general, to obtain high yields, a catalyst loading of 5 mol% is required and reactions need to be heated at more than 100 °C for 24 hours. To improve the reaction conditions, we synthesized a series of Ni(0), Ni(I), and Ni(II) precatalysts supported by either PCy_3 or the bidentate ligand dppf and tested their catalytic activity (see Table 1 for room temperature results and Table S1 for results at elevated temperature and additional precatalysts).[14m,16]

Our results for the coupling of naphthalen-1-yl dimethylsulfamate with 4-methoxyphenylboronic acid show that the most commonly used system in the literature,[10a,10c] $^{PCy}\mathbf{Ni}^{II}_{Cl2}$, is the least active of the precatalysts we tested (Entry 1 and Table S1). We suggest that this is in part due to its poor solubility at temperatures lower than 100 °C. In general, dppf-ligated Ni(II) and Ni(0) precatalysts are more active than their PCy_3-ligated counterparts (Entries 2 & 4 vs Entries 5 & 7). This trend is reversed for Ni(I) precatalysts and $^{PCy}\mathbf{Ni}^{I}_{Cl}$ is more active than $^{dppf}\mathbf{Ni}^{I}_{Cl}$ (Entry 3 vs 6). Although $^{dppf}\mathbf{Ni}^{I}_{Cl}$ is active, especially at elevated temperatures (Table S1), at room temperature it displays reduced activity compared to Ni(0) and Ni(II) species. In fact, $^{dppf}\mathbf{Ni}^{I}_{Cl}$ shows almost no activity at room temperature. This is in direct contrast to our previous work studying SMC reactions involving aryl chlorides, where $^{dppf}\mathbf{Ni}^{I}_{Cl}$ was highly active at room temperature,[15] and indicates that dppf-supported Ni(0) and Ni(II) precatalysts are not generating $^{dppf}\mathbf{Ni}^{I}_{Cl}$ as the active species in the coupling of aryl sulfamates.

The most active systems were $^{dppf}\mathbf{Ni}^{II}_{(o\text{-}tol)(Cl)}$ and $^{dppf2}\mathbf{Ni}^{0}$, which at 2.5 mol% catalyst loading quantitatively generated the product at room temperature (Entries 5 & 8). Remarkably, excellent conversion was even observed using only 1 mol% $^{dppf}\mathbf{Ni}^{II}_{(o\text{-}tol)(Cl)}$ at room temperature demonstrating the incredible activity of this precatalyst. We propose that the increased activity of $^{dppf}\mathbf{Ni}^{II}_{(o\text{-}tol)(Cl)}$ compared to the Ni(0) precatalyst, $^{dppf2}\mathbf{Ni}^{0}$, as well as the related system $^{dppf}\mathbf{Ni}^{0}_{C2H4}$, is due to its rapid activation (see below and SI).

Table 1. GC Yields (%) for PCy_3- and dppf-supported precatalysts for a SMC reaction involving a naphthyl sulfamate.

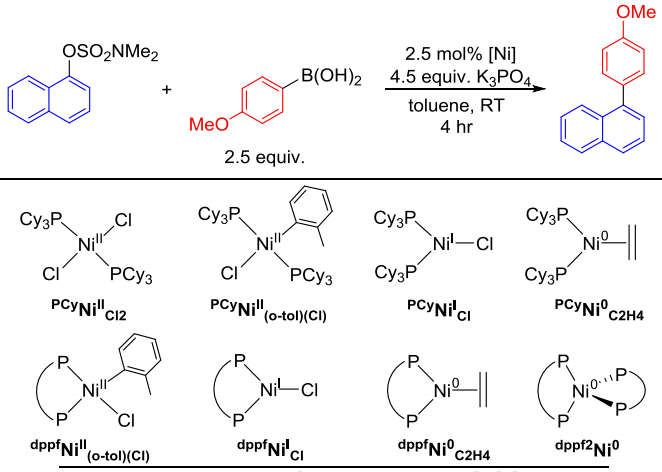

Entry	Precatalyst	Yield
1	$^{PCy}Ni^{II}_{Cl2}$	<1
2	$^{PCy}Ni^{II}_{(o\text{-}tol)(Cl)}$	55
3	$^{PCy}Ni^{I}_{Cl}$	50
4	$^{PCy}Ni^{0}_{C2H4}$	5
5	$^{dppf}Ni^{II}_{(o\text{-}tol)(Cl)}$	>99 (87)[a]
6	$^{dppf}Ni^{I}_{Cl}$	<1
7	$^{dppf}Ni^{0}_{C2H4}$	27 (<1)[a]
8	$^{dppf2}Ni^{0}$	>99 (39)[a]

Reaction conditions: 0.133 mmol naphthalene-1-yl dimethylsulfamate, 0.333 mmol 4-methoxyphenylboronic acid, 0.599 mmol K_3PO_4, 0.0665 mmol naphthalene (internal standard), 2.5 mol% precatalyst, and 1 mL toluene. Yields are the average of two runs and were determined using GC. [a] Yields in parentheses are for 1 mol% catalyst loading.

Substrate Scope

Using $^{dppf}Ni^{II}_{(o\text{-}tol)(Cl)}$ as the precatalyst, the substrate scope was explored (Table 2). Boronic acids containing both electron withdrawing and donating substituents were coupled in high yields with naphthalen-1-yl dimethylsulfamate at room temperature (Entries 1-5). When a di-*ortho*-substituted boronic acid (Entry 7) was used elevated temperature (60 °C) was required and the yield was slightly reduced. Rapid coupling at room temperature was also observed with naphthalen-2-yl dimethylsulfamate (Entry 10), although in the case of a naphthalen-2-yl dimethylsulfamate with an electron withdrawing group, longer reaction times were required to achieve high yields, due to the low solubility of the sulfamate in toluene (Entries 11 & 12). The reaction is compatible with a naphthalen-1-yl dimethylsulfamate with an electron donating moiety, but elevated temperature was required, presumably because oxidative addition is more challenging (Entry 13). Similarly, when either the boronic acid or naphthyl sulfamate contains heteroatoms, which are ubiquitous in pharmaceuticals,[17] elevated temperatures were necessary (Entries 6, 8, 9 & 14).

Table 2. Isolated yields for SMC reactions involving naphthyl sulfamate substrates using $^{dppf}Ni^{II}_{(o\text{-}tol)(Cl)}$ as the precatalyst.

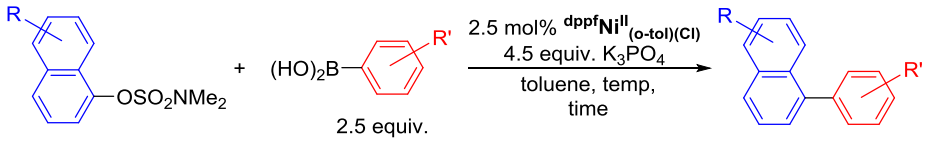

Entry	Sulfamate	Boronic Acid	Temp (°C)	Time (hr)	Yield
1	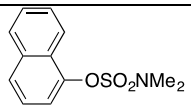	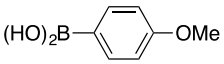	RT	4	95%
2	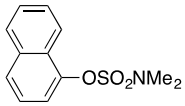	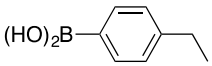	RT	4	85%
3	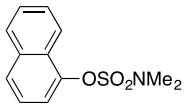	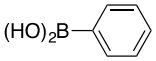	RT	4	88%
4	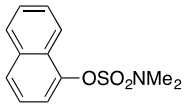	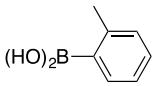	RT	4	92
5	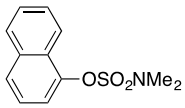	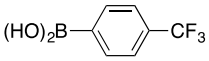	RT	24	79%
6	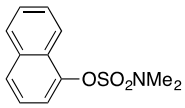	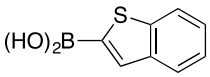	40	16	91%
7	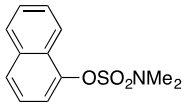	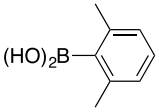	60	4	64
8	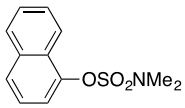	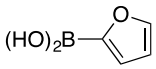	80	16	75%
9	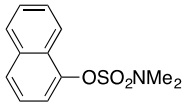	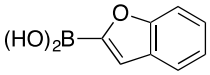	80	16	87%
10	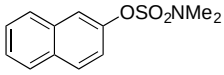	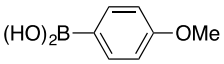	RT	4	84%
11	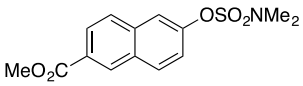	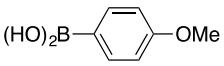	RT	24	90%
12	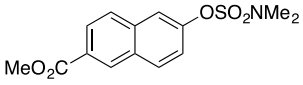	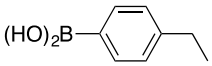	RT	24	93%
13	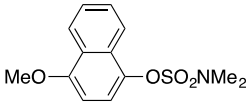	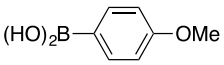	60	24	91%
14	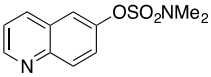	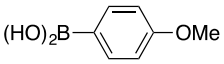	80	24	86%

Reaction conditions: 0.133 mmol naphthalenyl dimethylsulfamate, 0.333 mmol boronic acid, 0.599 mmol K_3PO_4, 2.5 mol% $^{dppf}Ni^{II}_{(o\text{-}tol)(Cl)}$, and 1 mL toluene. Yields are the average of two runs.

Table 3. Isolated yields for SMC coupling reactions involving phenyl sulfamate substrates using $^{dppf}Ni^{II}_{(o\text{-}tol)(Cl)}$ as the precatalyst.

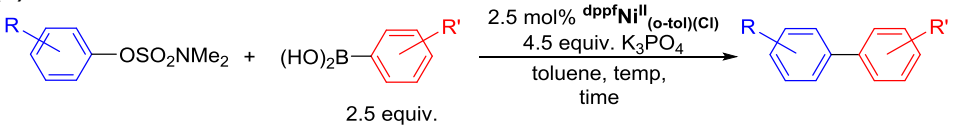

Entry	Sulfamate	Boronic Acid	Temp (°C)	Time (hr)	Yield
1	F_3C–OSO_2NMe_2	$(HO)_2B$–OMe	80	4	93%
2	OSO_2NMe_2	$(HO)_2B$–OMe	80	16	94%
3	OSO_2NMe_2	$(HO)_2B$–OMe	80	16	84%
4	MeO–OSO_2NMe_2	$(HO)_2B$–OMe	80	16	86%
5	F_3C–OSO_2NMe_2	$(HO)_2B$–	80	8	71%
6	OSO_2NMe_2	$(HO)_2B$–	80	18	75%
7	OSO_2NMe_2	$(HO)_2B$–	80	24	69%
8	MeO–OSO_2NMe_2	$(HO)_2B$–	80	24	72%
9	F_3C–OSO_2NMe_2	$(HO)_2B$–CF_3	80	24	73%
10	OSO_2NMe_2	$(HO)_2B$–CF_3	80	24	63%
11	MeO–OSO_2NMe_2	$(HO)_2B$–CF_3	80	24	58%
12	OSO_2NMe_2	$(HO)_2B$–	80	24	87%

Reaction conditions: 0.133 mmol phenyl dimethylsulfamate, 0.333 mmol boronic acid, 0.599 mmol K_3PO_4, 2.5 mol% $^{dppf}Ni^{II}_{(o\text{-}tol)(Cl)}$, and 1 mL toluene. Yields are the average of two runs.

The data in Table 3 show that the SMC reaction of phenyl sulfamates is more challenging than naphthyl sulfamates and elevated temperatures and slightly longer reaction times were required; however, the scope is still broad. As with naphthyl sulfamates, both electron deficient and rich electrophiles are tolerated (Entries 1, 4, 5, 8, 9 & 11). Notably, the precatalyst is compatible with sterically more demanding di-*ortho* substituted substrates (Entries 2 & 7). Significantly, the tri-

ortho substituted cross-coupled product, 2,2',6'-trimethylbiphenyl can be obtained in good yield (Entry 12). However, the tetra-*ortho* substituted analogue, 2,2',6,6'-tetramethylbiphenyl, could not be generated in appreciable yield. The efficiency of coupling of phenyl sulfamates was also significantly impacted by the electronic properties of the boronic acid. Reduced yields were obtained when using the more electron deficient phenylboronic acid and 4-trifluoromethylphenyl boronic acid (Entries 5-11) compared to the more electron rich 4-methoxyphenylboronic acid (Entries 1-4). Although we were able to couple quinoline electrophiles using $^{\mathbf{dppf}}\mathbf{Ni}^{\mathbf{II}}_{\mathbf{(o\text{-}tol)(Cl)}}$ (Table 2, Entry 12), we were not able to couple pyridyl derivatives under the same mild conditions.

The combined results in Tables 2 and 3 indicate that the most facile reactions occur between electron withdrawing sulfamates and electron donating boronic acids. This is consistent with previous observations that oxidative addition is easier for substrates with electron-withdrawing groups[18] and that boronic acids with electron-donating substituents are less likely to undergo protodeboronation.[19] Overall, the mild conditions that can be used with $^{\mathbf{dppf}}\mathbf{Ni}^{\mathbf{II}}_{\mathbf{(o\text{-}tol)(Cl)}}$ demonstrate that it generates a significantly better catalyst for the SMC reaction of aryl sulfamates and boronic acids than any other previously reported system.[10a,10c] In fact, its activity is comparable to the systems reported by Percec and co-workers for couplings between aryl sulfamates and neopentylglycolboronates,[10d,10g,10j] with the major advantage that boronic acids are readily available. Additionally, not only does $^{\mathbf{dppf}}\mathbf{Ni}^{\mathbf{II}}_{\mathbf{(o\text{-}tol)(Cl)}}$ exhibit remarkable efficiency as a precatalyst, but it is also a preferred system from a practical standpoint due to its facile preparation from inexpensive nickel salts, bench stability, and commercial availability.[20]

Precatalyst Activation and the Speciation of Nickel During Catalysis

To fundamentally understand the exceptional catalytic activity of $^{\mathbf{dppf}}\mathbf{Ni}^{\mathbf{II}}_{\mathbf{(o\text{-}tol)(Cl)}}$ and discern the factors that are important for the development of improved precatalysts, we performed mechanistic studies. It has previously been proposed that $^{\mathbf{dppf}}\mathbf{Ni}^{\mathbf{II}}_{\mathbf{(o\text{-}tol)(Cl)}}$ activates via initial transmetallation and subsequent reductive elimination to generate a putative catalytically active Ni(0) species[10c,15] but this process has not been studied under catalytic conditions. In a catalytic reaction between naphthalen-1-yl dimethylsulfamate and 4-methoxyphenylboronic acid, we quantified the amount of the activation product 2-methyl-4'-methoxybiphenyl and the cross-coupled product, 1-(4'-methoxyphenyl)naphthalene, as a function of time (Figure 2). Our results

indicate that activation of $^{dppf}\mathbf{Ni}^{II}_{(o\text{-}tol)(Cl)}$ is fast; within 15 minutes, the yield of 2-methyl-4'-methoxybiphenyl based on $^{dppf}\mathbf{Ni}^{II}_{(o\text{-}tol)(Cl)}$ is approximately 85%. The amount of 2-methyl-4'-methoxybiphenyl does not increase after 15 minutes and there is no $^{dppf}\mathbf{Ni}^{II}_{(o\text{-}tol)(Cl)}$ remaining after the reaction. This suggests that activation is not completely selective. Nevertheless, after 4 hours quantitative conversion to the cross-coupled product is observed. The same experiment was also conducted using 4-trifluoromethylphenyl sulfamate as the electrophile which, as shown in Table 3, is a substrate that requires elevated temperatures to achieve appreciable conversion. Quantifying the amount of the cross-coupled product 4-trifluoromethyl-4'-methoxybiphenyl and the amount of the activation product 2-methyl-4'-methoxybiphenyl at room temperature indicates that activation is still fast (~85% after 15 minutes), even when conversion to product is slow (Figure 2). In a similar fashion to the reaction using the naphthyl substrate, the maximum yield of 2-methyl-4'-methoxybiphenyl is 85% and there is no precatalyst present at the end of the reaction. This demonstrates that the same processes are likely occurring in activation regardless of whether a naphthyl or phenyl electrophile is utilized. Similarly, changing the boronic acid gives analogous results. When the reaction of unactivated phenylboronic acid, and naphthalen-1-yl dimethylsulfamate was monitored by GC, only ~70% of the activation product 2-methylbiphenyl was observed, despite essentially quantitative conversion to the cross-coupled product (see SI). Activation of the precatalyst is not affected when using the mono-*ortho* substituted 2-methylphenyl boronic acid, with approximately 87% of the activation product obtained (see SI). However, both activation of the precatalyst (~70%) and yield of cross-coupled product (57%) is decreased when using the di-*ortho* substituted 2,6-dimethylphenyl boronic acid (see SI).

One explanation for the observation of less than quantitative yields of the biphenyl activation products is that $^{dppf}\mathbf{Ni}^{II}_{(o\text{-}tol)(Cl)}$ undergoes a competing comproportionation reaction to initial transmetallation to generate Ni(I) species (Scheme 1).[13,15,21] To probe for Ni(I) formation, the speciation of nickel was investigated using EPR spectroscopy in the reaction of naphthalen-1-yl dimethylsulfamate and 4-methoxyphenylboronic acid using $^{dppf}\mathbf{Ni}^{II}_{(o\text{-}tol)(Cl)}$ as the precatalyst. An axial spectrum exhibiting hyperfine splitting consistent with two similar, but not identical phosphorus nuclei was observed both during and at the end of the reaction (Figure 3a). Quantification of the nickel at the end of the reaction indicated that 23% of the precatalyst was in an EPR active form (Figure 3a). Timecourse experiments (see SI) indicate that the quantity of

EPR active material increases throughout the reaction, showing that Ni(I) is formed while catalysis is occurring. Additionally, Ni(I) formation is not restricted to room temperature

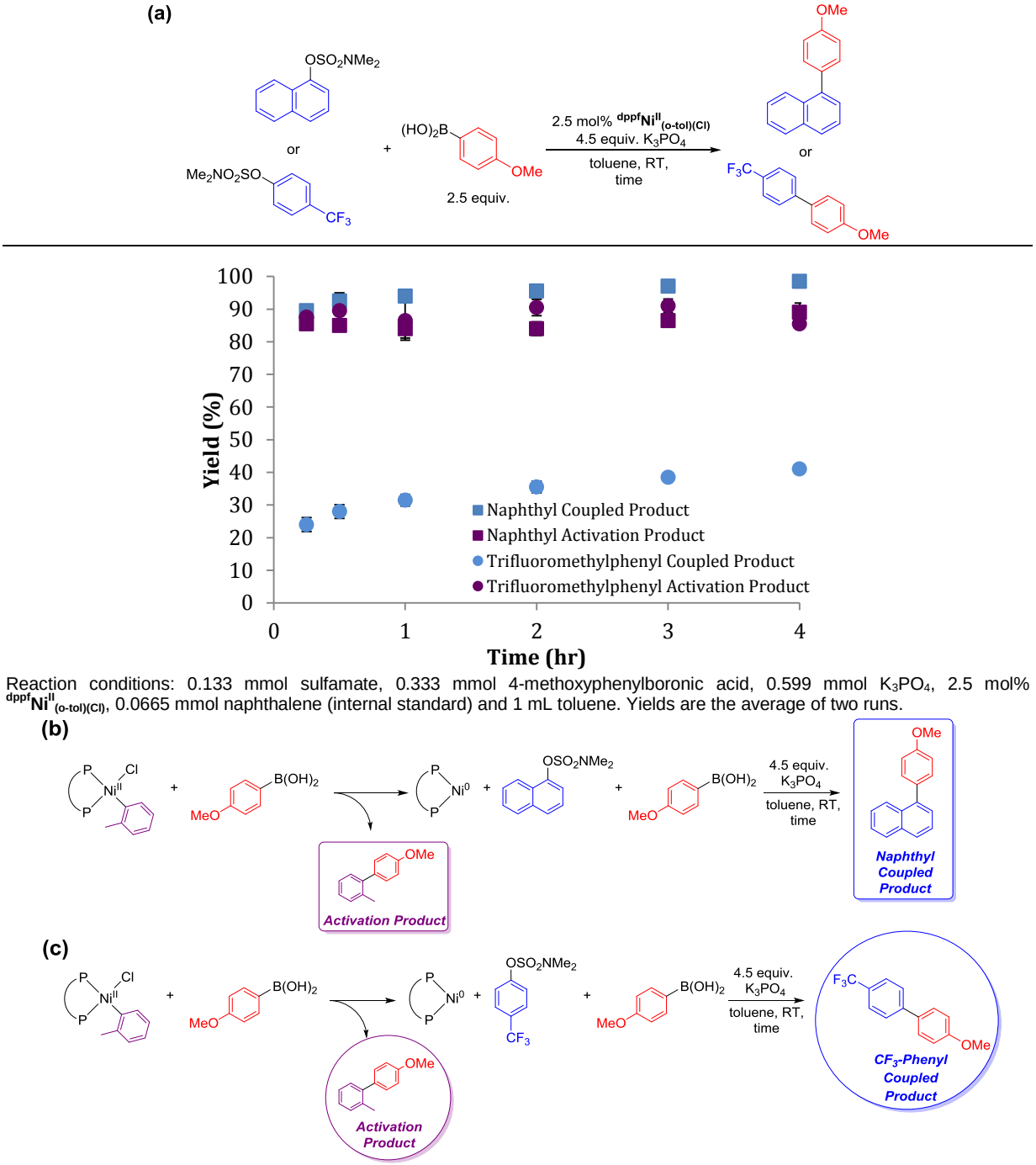

Reaction conditions: 0.133 mmol sulfamate, 0.333 mmol 4-methoxyphenylboronic acid, 0.599 mmol K_3PO_4, 2.5 mol% $^{dppf}Ni^{II}_{(o\text{-}tol)(Cl)}$, 0.0665 mmol naphthalene (internal standard) and 1 mL toluene. Yields are the average of two runs.

Figure 2. (a) Yield of cross-coupled and activation product as a function of time in selected SMC reactions using $^{dppf}Ni^{II}_{(o\text{-}tol)(Cl)}$. **(b)** & **(c)** Schematic showing formation of activation and cross-coupled products in reactions using naphthalen-1-yl dimethylsulfamate and 4-trifluoromethylphenyl sulfamate as the substrates.

reactions in toluene; the same phenomenon occurs at elevated temperature and in other solvents amenable to cross-coupling (see SI).

Comparison of the EPR spectra obtained in the reaction using $^{dppf}Ni^{II}_{(o\text{-}tol)(Cl)}$ as a precatalyst to an authentic spectrum of $^{dppf}Ni^{I}_{Cl}$ (shown in Figure 3c),[15,22] a potential product of comproportionation, indicates that they are not identical (see SI). The authentic $^{dppf}Ni^{I}_{Cl}$ spectrum has g values of 2.09 and 2.32, and two axial hyperfine values of [190, 150] and [220, 170] MHz arising from the ^{31}P nuclei.[15] However, the spectrum from catalysis using $^{dppf}Ni^{II}_{(o\text{-}tol)(Cl)}$ has less resolution in $g_{||}$ and the $g_{||}$ value also shifts to approximately 2.34 (see SI). Additionally, shouldering in the lineshape around 330 mT implies that another species is superimposed on the major contributor to the spectra; in fact, the spectra obtained in the reaction using $^{dppf}Ni^{II}_{(o\text{-}tol)(Cl)}$ as a precatalyst are consistent with the presence of multiple EPR active species.

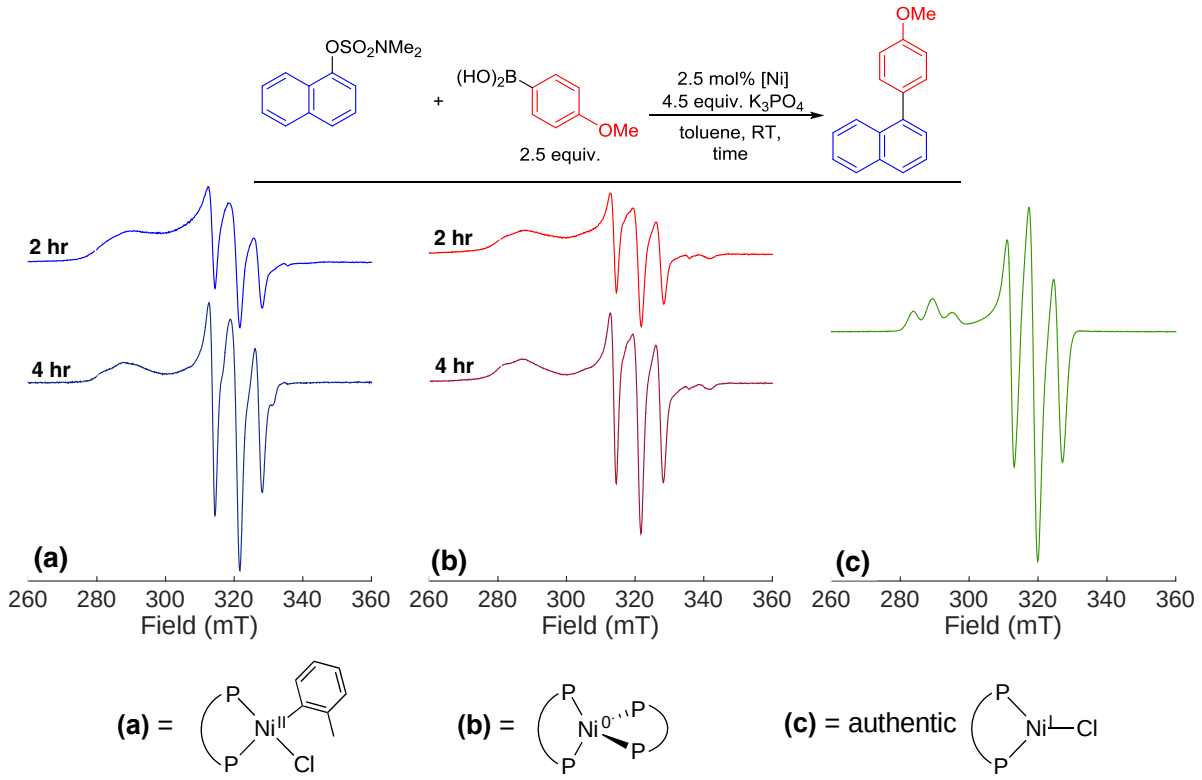

Figure 3. Low temperature X-band EPR spectra of catalytic mixtures from the SMC reaction of naphthalen-1-yl sulfamate and 4-methoxyphenylboronic acid catalyzed by $^{dppf}Ni^{II}_{(o\text{-}tol)(Cl)}$ **(a)** or $^{dppf2}Ni^{0}$ **(b)**. The spectrum in **(c)** is that of authentic $^{dppf}Ni^{I}_{Cl}$,[15] provided for comparison.

We propose that two Ni(I) species are present in detectable quantities in reactions using $^{dppf}\mathbf{Ni}^{II}_{(o\text{-}tol)(Cl)}$ as the precatalyst. One of these species is the known compound $^{dppf}\mathbf{Ni}^{I}_{Cl}$,[15,22] which is most likely formed via comproportionation between the unactivated $^{dppf}\mathbf{Ni}^{II}_{(o\text{-}tol)(Cl)}$ precatalyst and a dppf-supported Ni(0) species formed after activation of $^{dppf}\mathbf{Ni}^{II}_{(o\text{-}tol)(Cl)}$ (Scheme 1). Both our group and Schoenebeck and co-workers have previously synthesized $^{dppf}\mathbf{Ni}^{I}_{Cl}$ via comproportionation reactions,[15,22] which are well precedented for the formation of Ni(I) complexes even though the elementary steps are often unclear (*vide infra*).[13,14b,14f,14o,21,23] In our case the other product from comproportionation is the Ni(I) aryl species: $^{dppf}\mathbf{Ni}^{I}_{o\text{-}tol}$, which we do not directly observe. Stable three-coordinate Ni(I) aryl species are rare and limited to those with perfluorinated aryl groups;[24] as such, the Ni(I) aryl species generated through comproportionation in our reactions are expected to be unstable and degrade either through hydrogen abstraction or disproportionation followed by reductive elimination to yield mono- or biaryl organic species and Ni(0) species (see SI).[15,25] Organic products consistent with these processes were observed using GC in both catalytic and stoichiometric reactions (*vide infra*). It is likely that the Ni(0) species generated from Ni(I) aryl degradation can re-enter the catalytic cycle.[15]

We suggest that the other Ni(I) species detected by EPR spectroscopy in reactions using $^{dppf}\mathbf{Ni}^{II}_{(o\text{-}tol)(Cl)}$ as the precatalyst is $^{dppf}\mathbf{Ni}^{I}_{sulf}$, which we were unable to isolate. In this case, comproportionation between $^{dppf}\mathbf{Ni}^{II}_{(nap)(sulf)}$, generated via oxidative addition of the substrate, and a Ni(0) species would give rise to a Ni(I) sulfamate product, $^{dppf}\mathbf{Ni}^{I}_{sulf}$, and an unstable Ni(I) naphthyl species, $^{dppf}\mathbf{Ni}^{I}_{nap}$, as shown in Scheme 2. Indirect support for the formation of a Ni(I) sulfamate complex was provided by monitoring the catalytic reaction of naphthalen-1-yl dimethylsulfamate and 4-methoxyphenylboronic acid using $^{dppf2}\mathbf{Ni}^{0}$ as the precatalyst by EPR spectroscopy. Using this precatalyst, it is impossible to generate $^{dppf}\mathbf{Ni}^{I}_{Cl}$. Nevertheless, a clear signal attributed to $^{dppf}\mathbf{Ni}^{I}_{sulf}$ that accounts for 14% of the total nickel in solution is observed at the end of the reaction (Figure 3b). Timecourse experiments (see SI) indicate that the concentration of this species increases over the duration of the catalytic reaction. Using this authentic $^{dppf}\mathbf{Ni}^{I}_{sulf}$ spectrum as a guide, we modeled the EPR spectra observed when using $^{dppf}\mathbf{Ni}^{II}_{(o\text{-}tol)(Cl)}$ as the precatalyst as a linear combination of $^{dppf}\mathbf{Ni}^{I}_{Cl}$ and $^{dppf}\mathbf{Ni}^{I}_{sulf}$ (see SI). This provides a better model for the spectra than that obtained using only $^{dppf}\mathbf{Ni}^{I}_{Cl}$ or $^{dppf}\mathbf{Ni}^{I}_{sulf}$, as

ACS Paragon Plus Environment

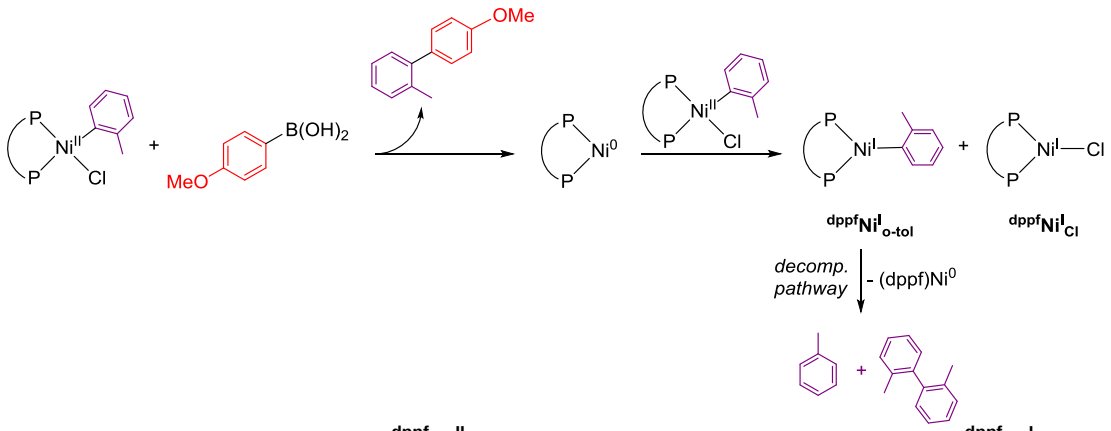

Scheme 1. Comproportionation of $^{dppf}\mathbf{Ni}^{II}_{(o\text{-}tol)(Cl)}$ with activated Ni(0) to produce $^{dppf}\mathbf{Ni}^{I}_{Cl}$ and aryl degradation products.

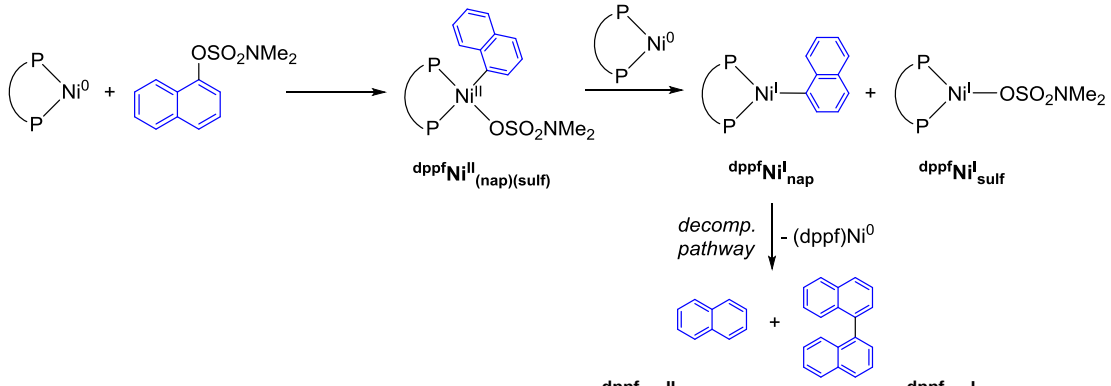

Scheme 2. Comproportionation of activated Ni(0) and $^{dppf}\mathbf{Ni}^{II}_{(nap)(sulf)}$ to produce $^{dppf}\mathbf{Ni}^{I}_{sulf}$ and naphthyl degradation products.

indicated by regression analysis. Furthermore, monitoring the reaction of naphthalen-1-yl sulfamate with 4-methoxyphenylboronic acid by EPR spectroscopy using $^{dppf}\mathbf{Ni}^{II}_{(o\text{-}tol)(Br)}$ (the Br analogue of $^{dppf}\mathbf{Ni}^{II}_{(o\text{-}tol)(Cl)}$) as the precatalyst also provides evidence for the presence of multiple EPR active species (see SI). In this case, hyperfine splitting from Br makes assignment more straightforward.

To further probe Ni(I) formation we performed stoichiometric reactions. These experiments are consistent with the pathway depicted in Scheme 3b, which involves a Ni(0)/Ni(II) catalytic cycle, with off-cycle processes to generate Ni(I) complexes. Initially, we treated $^{dppf}\mathbf{Ni}^{II}_{(o\text{-}tol)(Cl)}$ with naphthalen-1-yl dimethylsulfamate and 4-methoxyphenylboronic acid in the presence of 4.5 equivalents of K_3PO_4 (Scheme 3a), which generated the cross-coupled product 1-(4'-methoxyphenyl)naphthalene in 80% yield. In this reaction $^{dppf}\mathbf{Ni}^{II}_{(o\text{-}tol)(Cl)}$ is only 77% activated to Ni(0), as determined by the amount of 2-methyl-4'-methoxybiphenyl formed, while approximately 10% of the $^{dppf}\mathbf{Ni}^{II}_{(o\text{-}tol)(Cl)}$ remains unreacted. EPR spectroscopy indicates 13% of

the initial precatalyst undergoes comproportionation to form $^{dppf}Ni^{I}_{Cl}$ and $^{dppf}Ni^{I}_{o\text{-}tol}$. As discussed in Scheme 1 the latter is unstable and forms aryl degradation products. Consistent with this hypothesis we detected toluene and 2,2-dimethylbiphenyl by GC.

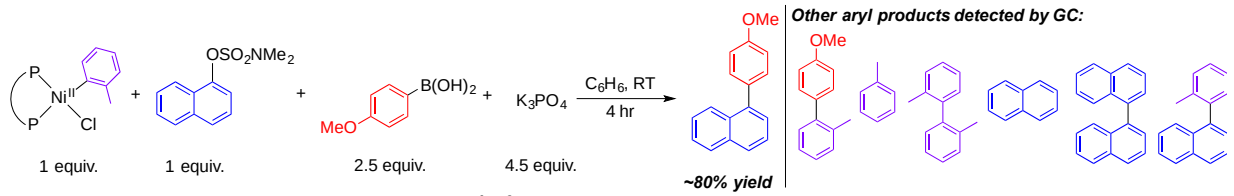

Scheme 3a. Stoichiometric reaction of $^{dppf}Ni^{II}_{(o\text{-}tol)(Cl)}$ with all catalytic components. Reaction conditions: 0.01352 mmol $^{dppf}Ni^{II}_{(o\text{-}tol)(Cl)}$, 0.01352 mmol sulfamate, 0.0338 mmol 4-methoxyphenylboronic acid, 0.599 mmol K_3PO_4, 0.0665 mmol 4,4'-dimethoxybiphenyl (internal standard) and 1 mL benzene.

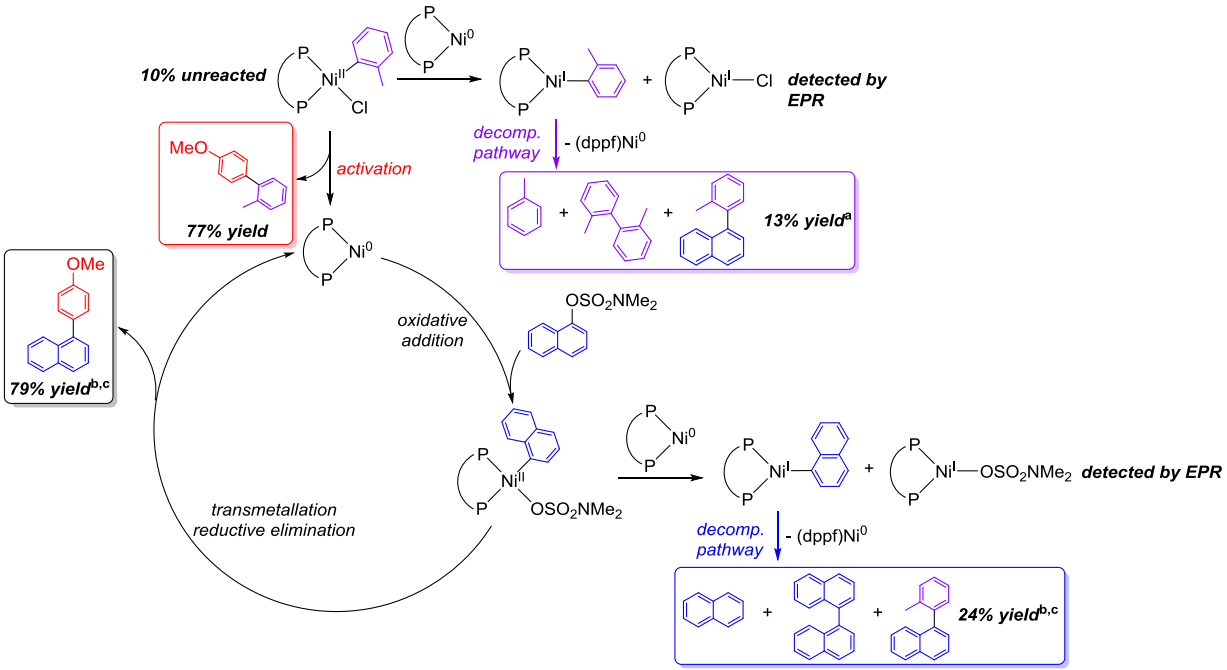

Scheme 3b. Proposed pathways of formation of aryl degradation products observed in stoichiometric reaction of $^{dppf}Ni^{II}_{(o\text{-}tol)(Cl)}$ with all catalytic components. [a]Quantification based on total moles of starting precatalyst. [b]Quantification based on sulfamate substrate as the limiting reagent.[c]Combined yield of these products exceeds 100% presumably due to the error associated with GC integrations. Organic products were quantified by GC, while nickel containing species were quantified using either NMR or EPR spectroscopy.

The organic products naphthalene and 1,1'-binaphthalene were also detected in 20% yield. We propose that they are formed from the decomposition of $^{dppf}Ni^{I}_{nap}$, which is one product from the comproportionation of $^{dppf}Ni^{II}_{(nap)(sulf)}$ with a Ni(0) species (see Scheme 2).[26] The other product of this comproportionation, $^{dppf}Ni^{I}_{sulf}$, was detected by EPR spectroscopy. The low yield of cross-coupled product (80%) is explained by the electrophile being consumed in the comproportination between $^{dppf}Ni^{II}_{(nap)(sulf)}$ and a Ni(0) species. In catalytic reactions this pathway would be expected to consume considerably less substrate due to the lower

concentration of nickel present in solution. In agreement with this hypothesis, yields approaching complete conversion to cross-coupled product are obtained in catalytic reactions where the catalyst loading is often only 2.5 mol% (see Tables 1, 2 & 3) but we still observe small amounts of the aryl products from degradation of $^{dppf}\mathbf{Ni}^{I}_{nap}$. Given the propensity of naphthyl electrophiles to exhibit markedly more activity than their phenyl counterparts,[3a] these experiments were repeated with phenyl electrophiles for congruency (see SI). The comproportionation phenomena seen with naphthyl electrophiles are also present in these reactions.

Additional evidence for the postulated $^{dppf}\mathbf{Ni}^{I}_{nap}$ and $^{dppf}\mathbf{Ni}^{I}_{sulf}$ complexes was obtained through a reaction between 0.5 equivalents of naphthalen-1-yl dimethylsulfamate and $^{dppf2}\mathbf{Ni}^{0}$ at room temperature (Scheme 4). After 24 hours 68% of the aryl sulfamate had reacted. EPR spectroscopy showed the generation of $^{dppf}\mathbf{Ni}^{I}_{sulf}$ and GC analysis indicated naphthyl degradation products consistent with $^{dppf}\mathbf{Ni}^{I}_{nap}$ formation and subsequent decomposition. Quantification of these organic products is also consistent with incomplete consumption of the aryl sulfamate and gives a 17% yield of naphthyl species based on $^{dppf2}\mathbf{Ni}^{0}$. This is in agreement, within error, with the 20% yield of $^{dppf}\mathbf{Ni}^{I}_{sulf}$ obtained using EPR spectroscopy. The results of this reaction are consistent with a model in which: (i) a Ni(I) sulfamate species is formed congruent with $^{dppf}\mathbf{Ni}^{I}_{nap}$; and (ii) this process occurs through comproportionation of activated Ni(0) with the Ni(II) oxidative addition intermediate $^{dppf}\mathbf{Ni}^{II}_{(nap)(sulf)}$. Further evidence in support of this model was obtained by changing the electrophile (see SI). As expected a substrate which underwent more facile oxidative addition generated less Ni(I), as in this case the Ni(0) species was relatively more likely to undergo oxidative addition compared to comproportionation.

In support of our competing off-cycle comproportionation model, a marked effect on Ni(I) formation was observed depending on the concentration of boronic acid (see SI). Our data indicate that higher boronic acid concentrations promote transmetallation of $^{dppf}\mathbf{Ni}^{II}_{(o\text{-}tol)(Cl)}$ and $^{dppf}\mathbf{Ni}^{II}_{(nap)(sulf)}$ before comproportionation can occur, facilitating productive catalysis by keeping more nickel in the catalytic cycle. When less boronic acid was used in catalytic reactions, precatalyst activation is decreased and the total amount of Ni(I) generated is increased, consistent with previous observations with aryl chloride electrophiles.[15] Furthermore, when using only 1.5 or 1.05 equivalents of boronic acid in stoichiometric reactions of $^{dppf}\mathbf{Ni}^{II}_{(o\text{-}tol)(Cl)}$, the yields of

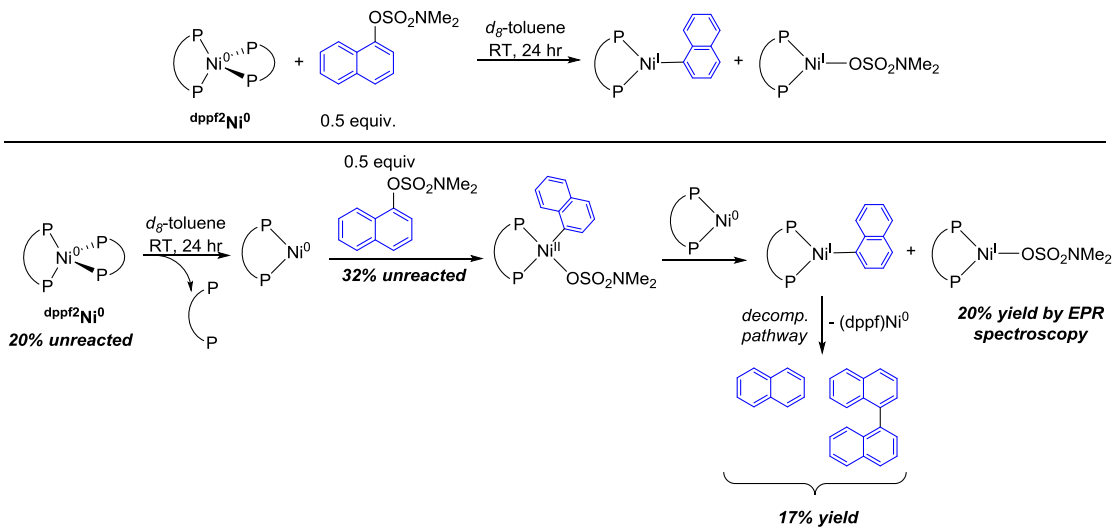

Scheme 4. Proposed route for Ni(I) formation via oxidative addition in the stoichiometric reaction of $^{dppf2}Ni^{0}$ with substrate. Quantification of aryl degradation products performed using GC with 2-(4'-methoxyphenyl)naphthalene as an internal standard. Yields based on total amount of precatalyst.

Table 4. Stoichiometric reactions using $^{dppf}Ni^{II}_{(o\text{-}tol)(Cl)}$ as a precatalyst for SMC reactions involving different numbers of equivalents of boronic acid.

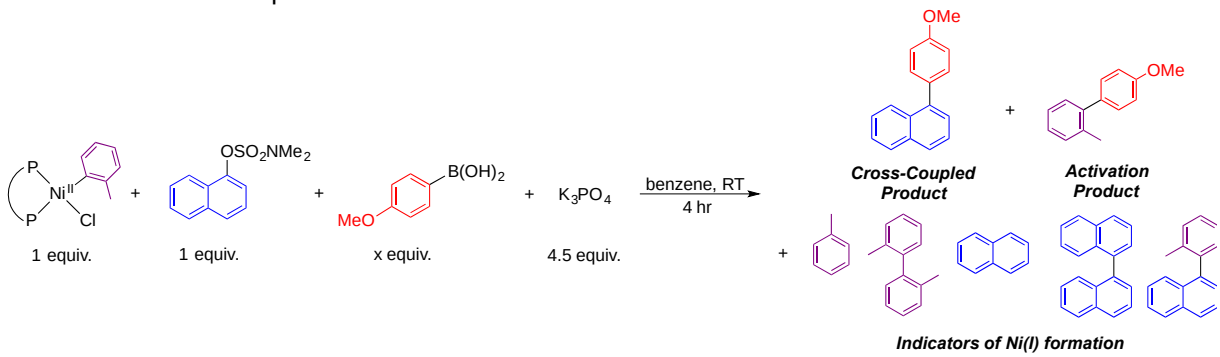

Equivalents Boronic Acid	Yield Cross-Coupled Product	Yield Activation Product	Total Yield Ni(I)[d] ($^{dppf}Ni^{I}_{sulf}$ and $^{dppf}Ni^{I}_{Cl}$)	Ratio $^{dppf}Ni^{I}_{sulf}$: $^{dppf}Ni^{I}_{Cl}$
2.5[a]	80%	77%	32% (36%)[e]	2:1
1.5[b]	51%	54%	45% (54%)[e]	1:2.5
1.05[c]	23%	35%	48% (62%)[e]	1:7

Reaction conditions: 0.01352 mmol $^{dppf}Ni^{II}_{(o\text{-}tol)(Cl)}$, 0.01352 mmol sulfamate, 0.0338[a], 0.0203[b], or 0.0142[c] mmol 4-methoxyphenylboronic acid, 0.599 mmol K_3PO_4, 0.0665 mmol 4,4'-dimethoxybiphenyl (internal standard) and 1 mL benzene. [d]Yield based on the total amount of precatalyst initially present. [e]Number in parenthesis is the yield based on the amount of precatalyst that was activated.

cross-coupled product and activation product are once again reduced (Table 4). Notably, the ratio of $^{dppf}Ni^{I}_{sulf}$ to $^{dppf}Ni^{I}_{Cl}$ decreases drastically upon using less boronic acid. This is quantified indirectly by comparing the total amount of naphthyl and binaphthyl degradation products formed (indicating the formation of $^{dppf}Ni^{I}_{sulf}$) to the total amount of phenyl and biphenyl degradation products formed (indicating the formation of $^{dppf}Ni^{I}_{Cl}$). The decrease in the ratio of $^{dppf}Ni^{I}_{sulf}$ to $^{dppf}Ni^{I}_{Cl}$ is also an artifact of a decrease in the rate of precatalyst activation, as this

causes an increase in the amount of $^{dppf}\mathbf{Ni}^{II}_{(o\text{-}tol)(Cl)}$ relative to $^{dppf}\mathbf{Ni}^{II}_{(nap)(sulf)}$. Consequently, Ni(0) is more likely to comproportionate with $^{dppf}\mathbf{Ni}^{II}_{(o\text{-}tol)(Cl)}$ to form $^{dppf}\mathbf{Ni}^{I}_{Cl}$ compared with $^{dppf}\mathbf{Ni}^{II}_{(nap)(sulf)}$ to form $^{dppf}\mathbf{Ni}^{I}_{sulf}$. As a result, the majority of the Ni(I) produced in the stoichiometric reaction using 1.05 equivalents of boronic acid is in the form of $^{dppf}\mathbf{Ni}^{I}_{Cl}$.

Overall, our results on the activation of $^{dppf}\mathbf{Ni}^{II}_{(o\text{-}tol)(Cl)}$ and its speciation during catalysis indicate that even under our optimized conditions, catalyst activation is not selective for Ni(0). The predominant reason for the less than quantitative activation of the precatalyst to Ni(0) is a comproportionation reaction between a Ni(0) species formed after activation and $^{dppf}\mathbf{Ni}^{II}_{(o\text{-}tol)(Cl)}$ to form an unstable Ni(I) aryl species and catalytically inactive $^{dppf}\mathbf{Ni}^{I}_{Cl}$. Increasing the rate of activation by increasing the concentration of boronic acid reduces the amount of $^{dppf}\mathbf{Ni}^{I}_{Cl}$ but it is still formed in detectable quantities under our optimized conditions and reduces catalyst performance. Furthermore, a second detrimental process that consumes substrate also occurs to generate Ni(I) species. In this pathway, Ni(0) undergoes comproportionation with $^{dppf}\mathbf{Ni}^{II}_{(Ar)(sulf)}$ to form an unstable Ni(I) aryl species and $^{dppf}\mathbf{Ni}^{I}_{sulf}$. Our results confirm that in a similar fashion to Negishi and Kumada reactions involving alkyl halides[14a,14d-f,14k,14o-q] and SMC reactions of aryl halides,[13,15] Ni(I) species are present in SMC reactions involving aryl sulfamates. However, in the latter case, unlike previous studies on the role of Ni(I) species in SMC reactions involving aryl halides,[13,15] the almost negligible catalytic activity of $^{dppf}\mathbf{Ni}^{I}_{Cl}$ at room temperature clearly establishes that the generation of this species is detrimental to catalysis; the first time it has definitively been established that Ni(I) formation needs to be avoided in a nickel-catalyzed SMC reaction. Our findings are also distinct from other nickel-catalyzed reactions where Ni(I) species are proposed to be inactive, such as Buchwald-Hartwig and trifluoromethylthiolation reactions,[22,25d] as in these cases there is no direct evidence that Ni(I) complexes are formed *in situ* during catalysis.

DFT Calculations on the Comproportionation of Ni(II) and Ni(0)

Our experimental results suggest that by suppressing comproportionation to generate Ni(I) complexes, we could generate improved precatalysts. This is difficult because the elementary steps in comproportionation are not well understood. In catalysis, the extent of comproportionation of $^{dppf}\mathbf{Ni}^{II}_{(o\text{-}tol)(Cl)}$ with Ni(0) to yield essentially inactive $^{dppf}\mathbf{Ni}^{I}_{Cl}$ depends on the relative rates of three different processes: (1) the activation of Ni(II) to Ni(0), (2) the

oxidative addition of the electrophile and (3) the comproportionation reaction itself (see Scheme 3b). Ni(0) catalysts do not involve process (1), but they still require activation; *e.g.*, the exchange of ethylene by toluene in $^{dppf}\mathbf{Ni}^{0}_{C2H4}$, which is endoergic by 15.7 kcal mol^{-1} (Figure S19). In contrast, Ni(II) activation involves transmetallation followed by reductive elimination.[15,27] Although transmetallation is proposed to be facile it is a difficult process to model due to a lack of understanding about the exact role of the base (K_3PO_4 in this case),[28] especially for nickel-catalyzed reactions in non-polar solvents such as toluene.[29] Furthermore, the speciation of K_3PO_4 in toluene is not clear, which complicates modeling, and the exact concentration of K_3PO_4 is unknown, resulting in problems obtaining accurate energies. Therefore, herein we focus on steps (2) and (3) by means of DFT calculations at the M06L-DZP/M06-TZP SMD(benzene) level,[30] which has been benchmarked against X-Ray structures and CCSD(T) energies (Tables S17-19 and Figure S18).[31]

Comproportionation was initially studied by optimizing both the Ni(II) precatalyst $^{dppf}\mathbf{Ni}^{II}_{(o\text{-}tol)(Cl)}$ and the coordinatively unsaturated Ni(0) complex, (dppf)Ni ($^{dppf}\mathbf{Ni}^{0}$), within a single "super-molecule" in the singlet state **S-dimer$_{Cl}$** (Figure 4 and 5). After assessing different conformations, it was found that in the most stable conformation the Ni(II) center is still in a square planar geometry with the dppf ligand bound in a bidentate fashion and the metal bound to both the *o*-tolyl and Cl ligands (Ni(1)-Cl(3) = 2.27 Å and Ni(1)-C(6) = 1.92 Å). The Ni(0) center adopts a distorted tetrahedral geometry with the metal weakly bound to the Cl ligand (Ni(2)-Cl(3) = 2.56 Å) and strongly bound to one of the delocalized C=C bonds of a phenyl ring of the dppf ligand coordinated to the Ni(II) center (the Ni(2)-C(4) and Ni(2)-C(5) distances are 2.05 and 2.09 Å, respectively). The phosphine ligand is thus playing an unexpected bridging role, which contributes to the exoergic formation of **S-dimer$_{Cl}$** from the separated $^{dppf}\mathbf{Ni}^{II}_{(o\text{-}tol)(Cl)}$ and (dppf)Ni(benzene) ($^{dppf}\mathbf{Ni}^{0}_{benz}$) complexes; ΔG = -6.2 kcal mol^{-1} (see Figure 5). The complex $^{dppf}\mathbf{Ni}^{0}_{benz}$ is used as the energy reference instead of naked $^{dppf}\mathbf{Ni}^{0}$, because the solvent, upon coordination, stabilizes the system by ~10 kcal mol^{-1} (see Eqs. S5 and S6 in the SI).

The transformation of the Ni(II)/Ni(0) core into a Ni(I)/Ni(I) core requires singlet-to-triplet spin crossover accompanied by the migration of the Cl ligand. This feature was explored by re-optimizing the geometry of **S-dimer$_{Cl}$** in the triplet state, which yielded **T-dimer$_{Cl}$** as an energy minimum (Figure 4 and Table S20). As expected, in this structure one metal is bound to the *o*-

ACS Paragon Plus Environment

tolyl ligand (Ni(1)-C(6) = 1.97 Å), whereas the other is bound to the Cl ligand (Ni(2)-Cl(3) = 2.23 Å), both in a distorted T-shaped coordination geometry. The bridging μ-Ph feature from the dppf ligand is not present in **T-dimer$_{Cl}$** (the Ni(2)-C(4) and Ni(2)-C(5) distances are now 3.58 and 3.63 Å, respectively) and the long Ni(1)···Cl(3) contact (3.08 Å) suggests that the Cl ligand does not connect the two Ni(I) centers either. The natural local spin densities (ρ) are consistent with the presence of two ferromagnetic-coupled Ni$^{\uparrow}$(I) centers; ρ(Ni) = 0.77 (*o*-tolyl-bound) and 0.85 (Cl-bound) *a.u.*. The free energy difference between **T-dimer$_{Cl}$** and **S-dimer$_{Cl}$** is only 1.2 kcal mol^{-1} in favor of the singlet state.

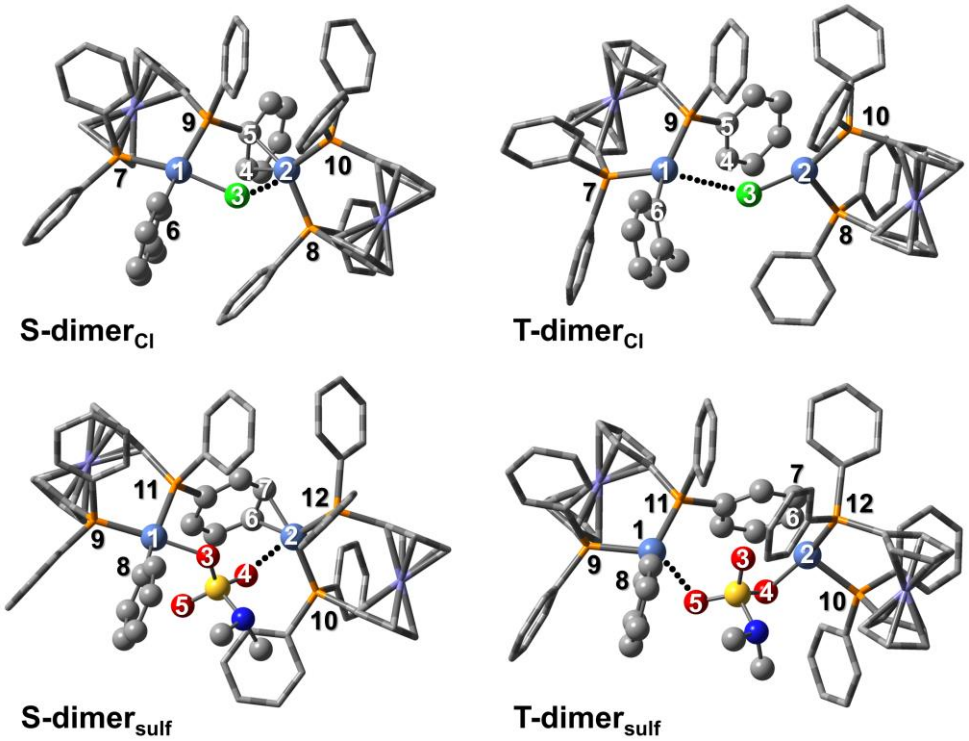

Figure 4. Fully optimized geometries of **S-dimer$_{Cl}$**, **T-dimer$_{Cl}$**, **S-dimer$_{sulf}$**, and **T-dimer$_{sulf}$**. For clarity, the dppf ligand is drawn in a "tube" representation, except for the phenyl ring interacting with nickel. Color code: Light blue (Ni), dark blue (N), green (Cl), grey (C), orange (P), lilac (Fe), red (O), yellow (S).

The kinetics of comproportionation were modeled using a relaxed energy scan (Figure S23). This scan shows how the potential energy of the system varies by freezing a set of internal coordinates at different values and allowing the remainder of the molecule to relax in a series of restrained geometry optimizations. These optimizations were performed for both the singlet and triplet states with the aim of finding a crossing point between them. Shortening of the Ni(2)-Cl(3) distance in the **S-dimer$_{Cl}$** geometry does not trigger the reaction – even when the Cl ligand is fully transferred to the Ni(2) center (Ni(2)-Cl(3) = 2.25 Å), the Ni(2) center remains strongly

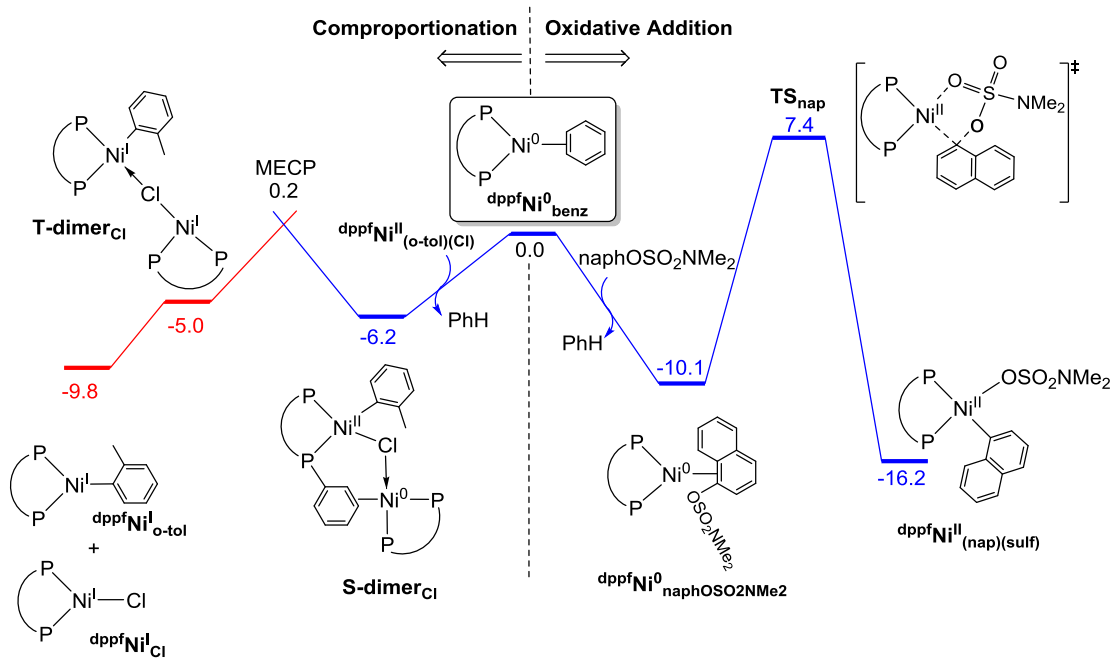

Figure 5. Singlet (blue) and triplet (red) free energy profiles in benzene in kcal mol^{-1} for the oxidative addition of naphthalene-1-yl dimethylsulfamate (naphOSO_2NMe_2) to ^{dppf}**Ni^0**$_{benz}$ (right) and comproportionation of ^{dppf}**Ni^0**$_{benz}$ with ^{dppf}**Ni^{II}**$_{(o\text{-}tol)(Cl)}$ (left). The energy for the MECP has been estimated by means of a relaxed energy scan (Figure S23).

bound to the phenyl ligand of the Ni(1)(dppf) moiety. Instead, the reaction is triggered by elongation of the Ni(2)-(C4=C5) π-bond distance. When the Ni(2)-C(5) bond distance was increased in sixteen +0.10 Å steps from 2.35 to 3.95 Å, the energy of the singlet state rises from 3.5 to 13.8 kcal mol^{-1} above **S-dimer$_{Cl}$**. When the Ni(2)-C(5) bond distance is 3.65 Å, the energy of the singlet state geometry (**S-dimer'$_{Cl}$**; Table S20), 12.2 kcal mol^{-1} above **S-dimer$_{Cl}$**, becomes lower upon re-optimization in the triplet state (**T-dimer'$_{Cl}$**), 11.7 kcal mol^{-1} above **S-dimer$_{Cl}$**. Energy refinement by thermochemistry corrections and basis set expansion reduce this spin crossover energy to 6.4 kcal mol^{-1} relative to **S-dimer$_{Cl}$**. The similar energies and geometrical parameters of **S-dimer'$_{Cl}$** and **T-dimer'$_{Cl}$** suggest that these structures are close to the minimum energy crossing point (MECP) between the two spin states. In line with this, their full optimization without any geometry or symmetry constraints in the singlet and triplet states yielded the expected **S-dimer$_{Cl}$** and **T-dimer$_{Cl}$** complexes, respectively. Both the dissociation of **T-dimer$_{Cl}$** into products, ^{dppf}**Ni^{I}**$_{Cl}$ and ^{dppf}**Ni^{I}**$_{o\text{-}tol}$, and the formation of the latter from the initial reactants, ^{dppf}**Ni^{II}**$_{(o\text{-}tol)(Cl)}$ and ^{dppf}**Ni^{0}**$_{benz}$, are thermodynamically favorable, with ΔG = -5.0 kcal mol^{-1} and -9.8 kcal mol^{-1}, respectively (see Figure 5). These data show that comproportionation between ^{dppf}**Ni^{II}**$_{(o\text{-}tol)(Cl)}$ and Ni(0) should be a facile low-barrier exoergic process and illustrate

the elementary steps involved. The calculations also showed that the Ni(I)-aryl product can yield the biaryl species observed experimentally (*vide supra*), because disproportionation to $^{dppf}\mathbf{Ni}^{II}_{(o\text{-}tol)2}$ and a Ni(0) species and the subsequent reductive elimination of 2,2'-dimethyl-1,1'-biphenyl are both exoergic (Figure S22).

Comproportionation was also studied from Ni(0) and $^{dppf}\mathbf{Ni}^{II}_{(nap)(sulf)}$, which was modelled using a phenyl ligand instead of a naphthyl ligand ($^{dppf}\mathbf{Ni}^{II}_{(ph)(sulf)}$) (Figure 6). The singlet state dimer of this system (**S-dimer**$_{sulf}$), shows that Ni(II) and Ni(0) are bridged by two oxygens of the sulfamate anion (O(3) and O(4)). In addition, the Ni(0) center is stabilized by the π-η^2 coordination of a phenyl ring of the dppf ligand bound to Ni(II). Similar to **S-dimerCl**, these interactions contribute to the exergonic formation of **S-dimer**$_{sulf}$ from $^{dppf}\mathbf{Ni}^{II}_{(ph)(sulf)}$ + $^{dppf}\mathbf{Ni}^{0}_{benz}$; ΔG = -7.4 kcal mol^{-1}. The formation of the triplet state dimer (**T-dimer**$_{sulf}$), which is almost isoenergetic to **S-dimer**$_{sulf}$, is also exergonic by -8.0 kcal mol^{-1}. The structure of this species contains two distorted T-shaped Ni(I) centers, one bound to the phenyl and the other to the sulfamate (Figure S24). As in the chloride system, the singlet-to-triplet spin crossover, which was also investigated by means of a relaxed energy scan (Figure S24), requires the elongation of the Ni(2)-C(6)=C(7) bond. In this case, at 2.45 Å, the triplet state energy becomes lower than that of the singlet by 1.7 kcal mol^{-1}. Upon adding the thermochemistry corrections and refining the energy, this approximate MECP structure stands 1.6 kcal mol^{-1} above **S-dimer**$_{sulf}$ (-5.8 kcal mol^{-1} below the initial reactants). Overall, after dissociation of **T-dimer**$_{sulf}$ into $^{dppf}\mathbf{Ni}^{I}_{ph}$ + $^{dppf}\mathbf{Ni}^{I}_{sulf}$,[32] comproportionation is exergonic by -15.8 kcal mol^{-1} and becomes more favorable when the phenyl ring is replaced by naphthyl (ΔG = -18.5 kcal mol^{-1}). The structure and energy data compiled in Figures 4-6 suggests that comproportionation to Ni(I) is a facile low-barrier exoergic process, which, for both the chloride and sulfamate systems, seems to be favored by the interaction between nickel and a dppf phenyl. In line with this, the re-optimization of the comproportionation pathway without this interaction in the sulfamate system yield a higher MECP with an energy of 9.5 kcal mol^{-1} above $^{dppf}\mathbf{Ni}^{0}_{benz}$ + $^{dppf}\mathbf{Ni}^{II}_{(ph)(sulf)}$.

The oxidative addition of naphthalene-1-yl dimethylsulfamate (naphOSO$_2$NMe$_2$) to $^{dppf}\mathbf{Ni}^{0}_{benz}$ was calculated for comparison with the comproportionation energy barriers (Figure 5). Substitution of the coordinated solvent benzene by naphOSO$_2$NMe$_2$ is exergonic by 10.1 kcal

ACS Paragon Plus Environment

mol^{-1}. From this species, the oxidative addition has an energy barrier of 17.5 kcal mol^{-1} and it proceeds through a transition state containing a 5-membered ring. Calculations on the alternative 3-membered ring transition state suggested that this involves a higher energy barrier ($\Delta G^{\ddagger}$ > 29 kcal mol^{-1}, see SI). The proposed pathway is consistent with others that have been calculated for related systems.[10c,33] A similar pathway was also calculated for oxidative addition of phenyl sulfamate ($phOSO_2NMe_2$, see Figure S25). Formation of the final $^{dppf}\mathbf{Ni}^{II}_{(nap)(sulf)}$ product is exergonic by 16.2 kcal mol^{-1}. In contrast, oxidative addition to $^{dppf}\mathbf{Ni}^{I}_{Cl}$ is strongly endoergic by 28.5 kcal mol^{-1} (Figure S20). Comparison of the energy profiles depicted in Figures 5 and 6 for oxidative addition and comproportionation suggest that the latter is kinetically preferred, consistent with the off-cycle processes proposed for $^{dppf}\mathbf{Ni}^{II}_{(o\text{-}tol)(Cl)}$ and $^{dppf}\mathbf{Ni}^{II}_{(nap)(sulf)}$ in Scheme 3b. Indeed, the low spin-crossover barriers for comproportionation make this process competitive even with oxidative addition of aryl chloride substrates, which have a lower energy barrier than aryl sulfamates (Figure S26). This is consistent with experimental observations that $^{dppf}\mathbf{Ni}^{I}_{Cl}$ is formed in SMC reactions with aryl chlorides using $^{dppf}\mathbf{Ni}^{II}_{(o\text{-}tol)(Cl)}$ as the precatalyst.[15] However, it should be noted that in all these systems, the concentration of substrate is far greater than the concentration of nickel, which increases the likelihood of oxidative addition over comproportionation.

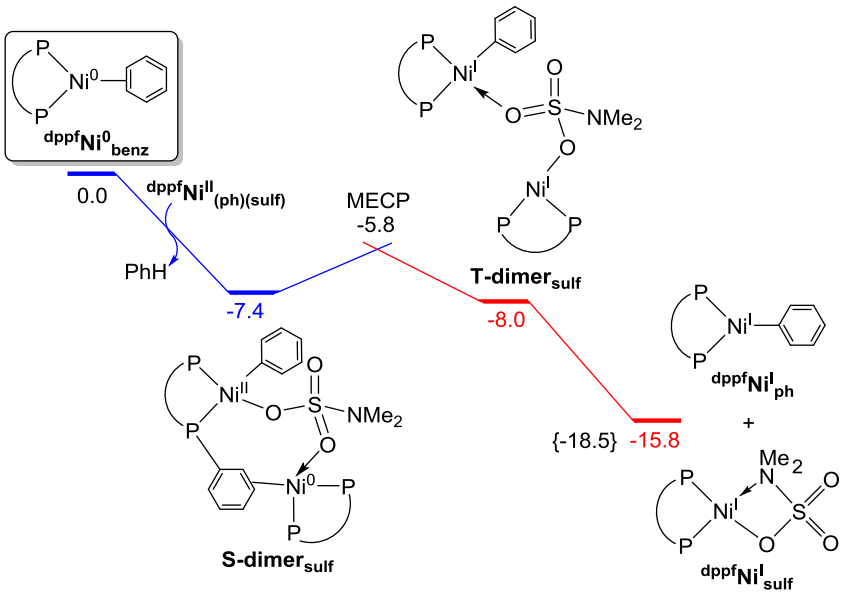

Figure 6. Free energy profile in benzene in kcal mol^{-1} for the comproportionation of $^{dppf}\mathbf{Ni}^{0}_{benz}$ and $^{dppf}\mathbf{Ni}^{II}_{(ph)(sulf)}$. The energy for the MECP between the singlet (blue) and triplet (red) energy profiles has been estimated by means of a relaxed energy scan (Figure S24). The thermochemistry found for comproportionation starting from $^{dppf}\mathbf{Ni}^{II}_{(nap)(sulf)}$ instead of $^{dppf}\mathbf{Ni}^{II}_{(ph)(sulf)}$ is given in brackets.

Probing the Active Species in Catalysis using $^{dppf}Ni^{I}_{Cl}$

Improving the catalytic activity of Ni(I) species such as $^{dppf}\mathbf{Ni}^{\mathbf{I}}_{\mathbf{Cl}}$ could provide an alternative strategy to increase precatalyst performance, as then formation of Ni(I) complexes would be less problematic. Although a poor precatalyst at room temperature, $^{dppf}\mathbf{Ni}^{\mathbf{I}}_{\mathbf{Cl}}$ is a competent precatalyst for SMC reactions of aryl sulfamates at elevated temperature suggesting that this approach is feasible (Table S1). However, the pathway for activation of $^{dppf}\mathbf{Ni}^{\mathbf{I}}_{\mathbf{Cl}}$ and the intermediates during catalysis at elevated temperature are unknown, preventing rational improvements. There is no detectable reaction between $^{dppf}\mathbf{Ni}^{\mathbf{I}}_{\mathbf{Cl}}$ and 1 equivalent of the electrophile naphthalen-1-yl sulfamate; however, a relatively slow reaction occurs with the nucleophile 4-methoxyphenylboronic acid in the presence of base at elevated temperature (see SI). In this reaction, diamagnetic species are formed, implying that the Ni(I) complex can form closed-shell Ni complexes under the catalytic conditions. Although the exact speciation of the products is currently unclear, this reactivity is consistent with the similar trends in catalytic performance observed for precatalysts in the Ni(0), Ni(I), and Ni(II) oxidation state (*vide infra).* Furthermore, in a stoichiometric experiment containing $^{dppf}\mathbf{Ni}^{\mathbf{I}}_{\mathbf{Cl}}$, 1 equivalent naphthalen-1-yl sulfamate, 2.5 equivalents 4-methoxyphenylboronic acid, and 4.5 equivalents of K_3PO_4, cross-coupled product is observed (see SI), along with, a very small amount of organic by-products consistent with the presence of a Ni(I) naphthyl species, such as $^{dppf}\mathbf{Ni}^{\mathbf{I}}_{\mathbf{nap}}$. This suggests that some of the comproportionation processes that are operative in the $^{dppf}\mathbf{Ni}^{\mathbf{II}}_{\mathbf{(o\text{-}tol)(Cl)}}$ cycle may be applicable here as well.

The efficiency of $^{dppf}\mathbf{Ni}^{\mathbf{I}}_{\mathbf{Cl}}$ as a precatalyst is heavily influenced by the ease at which substrates undergo oxidative addition. Previous studies have demonstrated that phenyl halides are more difficult to oxidatively add than naphthyl halides,[3a] though aryl halides in general are more likely to undergo oxidative addition compared to aryl sulfamates.[3c] We compared the GC yields of cross-coupled product using $^{dppf}\mathbf{Ni}^{\mathbf{I}}_{\mathbf{Cl}}$ as a precatalyst at 50 °C for 4 hours for the SMC reactions of 1-chloronaphthalene, naphthalen-1-yl sulfamate and 4-trifluoromethylphenyl sulfamate with 4-methoxyphenylboronic acid (Scheme 5). The yield of product with 4-trifluoromethylphenyl sulfamate was only 9%, while when naphthalen-1-yl sulfamate was used as the substrate a 24% yield was obtained. Both of these are vastly inferior to 1-chloronaphthalene, which gave a yield of 90%. The trend in yields based on the difficulty of oxidative addition parallels that seen when using $^{dppf}\mathbf{Ni}^{\mathbf{II}}_{\mathbf{(o\text{-}tol)(Cl)}}$ as a precatalyst (as indicated by the substrate scope), as well as when using

$^{dppf2}Ni^{0}$ as a precatalyst (see SI), which may imply that the same catalytically active species play a role in the catalytic cycle using $^{dppf}Ni^{I}_{Cl}$ and $^{dppf}Ni^{II}_{(o\text{-}tol)(Cl)}$.

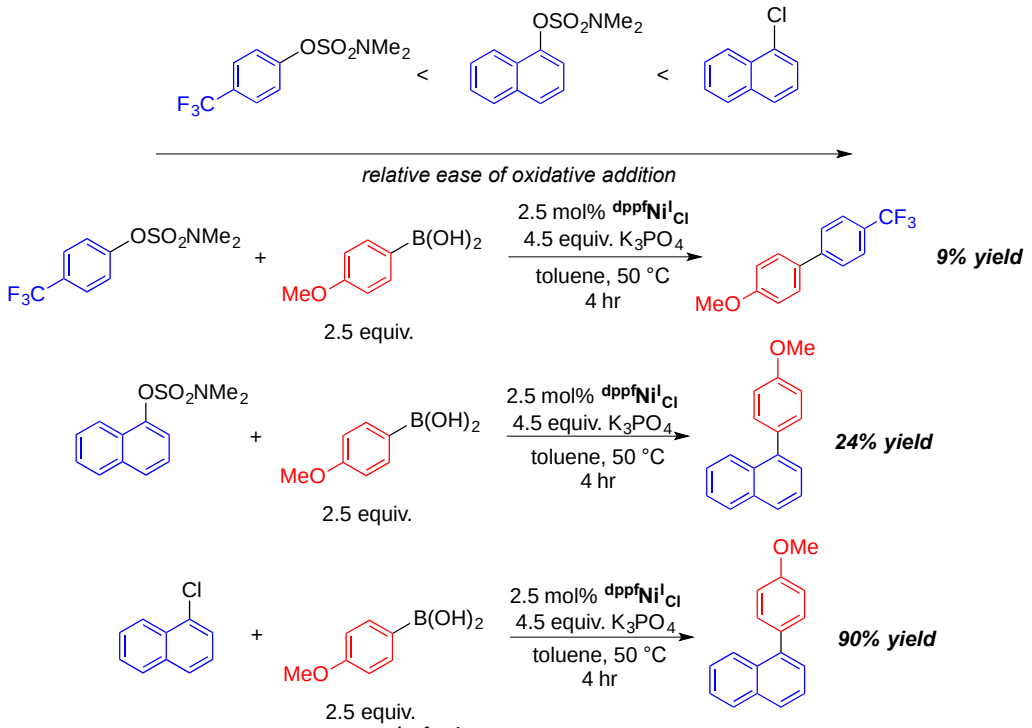

Scheme 5. SMC reactions catalyzed by $^{dppf}Ni^{I}_{Cl}$ using substrates that are increasingly more difficult to oxidatively add.

To further assess whether catalysis using $^{dppf}Ni^{I}_{Cl}$ proceeds through similar intermediates to $^{dppf}Ni^{II}_{(o\text{-}tol)(Cl)}$, a preferential product formation reaction in which sulfamate substrates with opposite electronic properties were coupled with only 1 equivalent of boronic acid catalyzed by 2.5 mol% of $^{dppf}Ni^{II}_{(o\text{-}tol)(Cl)}$, $^{dppf}Ni^{I}_{Cl}$, or $^{dppf2}Ni^{0}$ at 80 °C for 24 hours was performed (Scheme 6). Comparison of the resulting ratio of cross-coupled products formed provides evidence on the mechanisms of each precatalyst – if the ratios are similar, then the precatalysts most likely operate through similar intermediates, implying a similar catalytic cycle. However, if the ratios are drastically different, the catalytic cycles may be distinct from one another. The results indicate that, within error, the Ni(II), Ni(I), and Ni(0) systems give the same ratio of products, with preference for the electron-withdrawing cross-coupled product. This suggests that, regardless of the starting oxidation state of the precatalyst, the intermediates in the catalytic cycle are potentially similar.

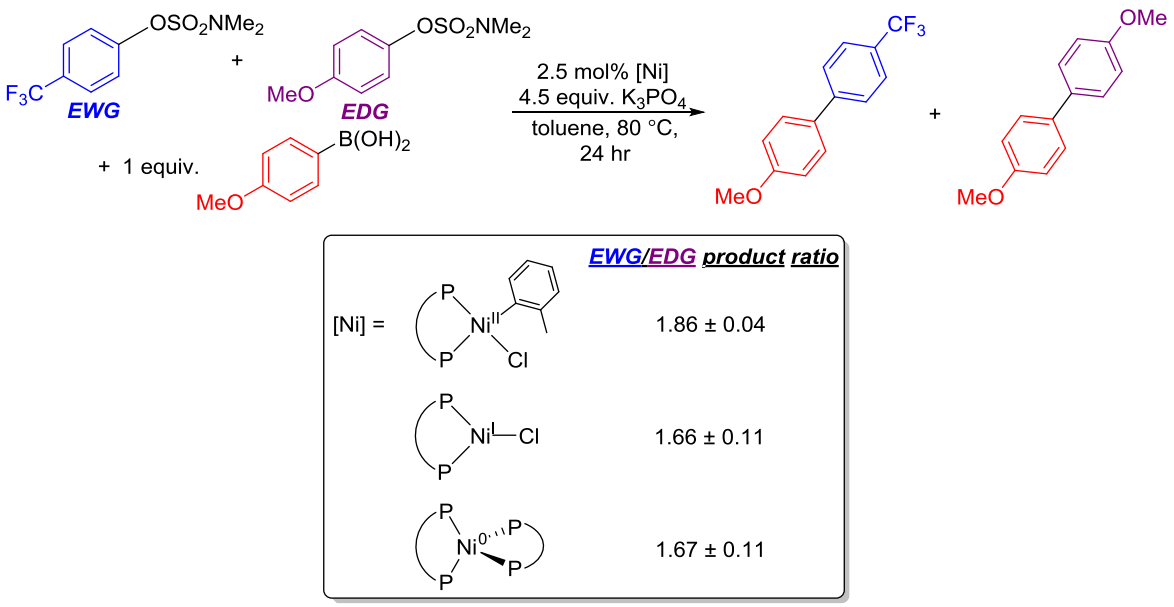

Scheme 6. Preferential product formation for SMC reactions catalyzed by $^{dppf}Ni^{II}_{(o\text{-}tol)(Cl)}$, $^{dppf}Ni^{I}_{Cl}$, or $^{dppf2}Ni^{0}$ with aryl sulfamates of differing electronic properties and only one equivalent of boronic acid. Ratios are the average of two runs with naphthalene as an internal standard.

All of our current evidence indicates that $^{dppf}Ni^{I}_{Cl}$ is forming the same active catalyst as $^{dppf}Ni^{II}_{(o\text{-}tol)(Cl)}$. We suggest that $^{dppf}Ni^{I}_{Cl}$ can be converted to diamagnetic species (Ni(0) or Ni(II)) in the presence of boronic acid and base, which can subsequently enter the same catalytic cycle as that of $^{dppf}Ni^{II}_{(o\text{-}tol)Cl.}$. With substrates that undergo rapid oxidative addition the Ni(0) species is more likely to enter into the Ni(0)/Ni(II) catalytic cycle rather than comproportionate back to Ni(I). This explains why the catalytic activity of $^{dppf}Ni^{I}_{Cl}$ is dependent on the electrophile and is consistent with the observation that aryl chlorides undergo coupling at room temperature[15] whereas aryl sulfamates are only reactive at elevated temperature. At this stage it is unclear whether activation of $^{dppf}Ni^{I}_{Cl}$ occurs via disproportionation into Ni(0) and Ni(II) species, via direct transmetallation to a Ni(I) aryl, followed by decomposition to a Ni(0) complex or through an alternative pathway. In future work, we will explore this process in more detail, which may lead to the development of improved Ni precatalysts.

Conclusions

We have shown that $^{dppf}Ni^{II}_{(o\text{-}tol)(Cl)}$ is a highly active precatalyst for SMC reactions involving aryl sulfamates. This system is so active that it can couple some substrates using low catalyst loading at room temperature. Mechanistic studies reveal that part of the reason for the high activity of $^{dppf}Ni^{II}_{(o\text{-}tol)(Cl)}$ is that it undergoes rapid activation to Ni(0). However, the reduction to

Ni(0) is not completely selective and some of the Ni(I) complex, $^{dppf}\mathbf{Ni}^{I}_{Cl}$, is formed via comproportionation during the activation process. Although $^{dppf}\mathbf{Ni}^{I}_{Cl}$ is catalytically active at elevated temperature, it is not as active as $^{dppf}\mathbf{Ni}^{II}_{(o\text{-}tol)(Cl)}$, and therefore the suppression of Ni(I) formation should result in more active precatalysts. Computational studies reveal that a key step in the generation of $^{dppf}\mathbf{Ni}^{I}_{Cl}$ is the formation of a dinuclear species that contains a bridging dppf ligand. In this complex, one of the nickel centers binds to the phenyl ring of dppf, which suggests that the modification of the ligand to prevent bridge formation may be a viable strategy to prevent the generation of $^{dppf}\mathbf{Ni}^{I}_{Cl}$. Our studies also reveal that a second Ni(I) species, $^{dppf}\mathbf{Ni}^{I}_{sulf}$, is formed during catalysis using $^{dppf}\mathbf{Ni}^{II}_{(o\text{-}tol)(Cl)}$. This species is also formed via a comproportionation reaction between Ni(0) and Ni(II) species. Preventing this process from occurring is also likely to result in more active systems, as this off-cycle reaction requires both active nickel species and the electrophile. Overall, even though we report a highly active precatalyst, our results show that there is significant room for further precatalyst improvement. This will be the goal of future research in our laboratory.

Acknowledgements

NH acknowledges support from the NSF through Grant CHE-1150826 and NIHGMS under Award Number R01GM120162. DB and AN acknowledge support from the Norwegian Research Council through the Center of Excellence for Theoretical and Computational Chemistry (CTCC) (Grant No. 179568/V30) and the Norwegian Metacenter for Computational Science (NOTUR; Grant nn4654k). DB also thanks the EU REA for a Marie Curie Fellowship (Grant CompuWOC/618303). AN thanks the Norwegian Research Council for the grants 221801/F20 and 250044/F20. MM thanks the NSF for support as an NSF Graduate Research Fellow. The EPR spectroscopy work was supported by the Department of Energy, Office of Basic Energy Sciences, Division of Chemical Sciences grant DE-FG02-05ER15646 (GWB and DJV). NH is a Camille and Henry-Dreyfus Foundation Teacher Scholar. We thank Professors James M. Mayer and Nathan D. Schley for valuable discussions and Dr. Brandon Q. Mercado for assistance with X-ray crystallography.

Supporting information available

Full characterizing data and experimental and computational procedures are available free of charge via the Internet at http://pubs.acs.org.

References

1. Miyaura, N.; Suzuki, A. *Chem. Rev.* **1995**, *95*, 2457.
2. Li, H. B.; Seechurn, C. C. C. J.; Colacot, T. J. *ACS Catal.* **2012**, *2*, 1147.
3. (a) Rosen, B. M.; Quasdorf, K. W.; Wilson, D. A.; Zhang, N.; Resmerita, A.-M.; Garg, N. K.; Percec, V. *Chem. Rev.* **2010**, *111*, 1346; (b) Hu, X. *Chem. Sci.* **2011**, *2*, 1867; (c) Han, F. S. *Chem. Soc. Rev.* **2013**, *42*, 5270; (d) Tasker, S. Z.; Standley, E. A.; Jamison, T. F. *Nature* **2014**, *509*, 299; (e) Ananikov, V. P. *ACS Catal.* **2015**, *5*, 1964; (f) Shields, J. D.; Gray, E. E.; Doyle, A. G. *Org. Lett.* **2015**, *17*, 2166; (g) Magano, J.; Monfette, S. *ACS Catal.* **2015**, *5*, 3120; (h) Malineni, J.; Jezorek, R. L.; Zhang, N.; Percec, V. *Synthesis* **2016**, *48*, 2795.
4. Yu, D.-G.; Yu, M.; Guan, B.-T.; Li, B.-J.; Zheng, Y.; Wu, Z.-H.; Shi, Z.-J. *Org. Lett.* **2009**, *11*, 3374.
5. Blakey, S. B.; MacMillan, D. W. C. *J. Am. Chem. Soc.* **2003**, *125*, 6046.
6. (a) Graham, T. J. A.; Shields, J. D.; Doyle, A. G. *Chem. Sci.* **2011**, *2*, 980; (b) Sylvester, K. T.; Wu, K.; Doyle, A. G. *J. Am. Chem. Soc.* **2012**, *134*, 16967; (c) Shields, J. D.; Ahneman, D. T.; Graham, T. J. A.; Doyle, A. G. *Org. Lett.* **2014**, *16*, 142.
7. Tobisu, M.; Xu, T.; Shimasaki, T.; Chatani, N. *J. Am. Chem. Soc.* **2011**, *133*, 19505.
8. (a) Saito, B.; Fu, G. C. *J. Am. Chem. Soc.* **2007**, *129*, 9602; (b) Saito, B.; Fu, G. C. *J. Am. Chem. Soc.* **2008**, *130*, 6694; (c) Wilsily, A.; Tramutola, F.; Owston, N. A.; Fu, G. C. *J. Am. Chem. Soc.* **2012**, *134*, 5794; (d) Zultanski, S. L.; Fu, G. C. *J. Am. Chem. Soc.* **2013**, *135*, 624.
9. (a) Percec, V.; Bae, J. Y.; Hill, D. H. *J. Org. Chem.* **1995**, *60*, 1060; (b) Zim, D.; Lando, V. R.; Dupont, J.; Monteiro, A. L. *Org. Lett.* **2001**, *3*, 3049; (c) Percec, V.; Golding, G. M.; Smidrkal, J.; Weichold, O. *J. Org. Chem.* **2004**, *69*, 3447; (d) Tang, Z.-Y.; Hu, Q.-S. *J. Am. Chem. Soc.* **2004**, *126*, 3058; (e) Hansen, A. L.; Ebran, J.-P.; Gøgsig, T. M.; Skrydstrup, T. *J. Org. Chem.* **2007**, *72*, 6464; (f) Tobisu, M.; Shimasaki, T.; Chatani, N. *Angew. Chem. Int. Ed.* **2008**, *47*, 4866; (g) Quasdorf, K. W.; Tian, X.; Garg, N. K. *J. Am. Chem. Soc.* **2008**, *130*, 14422; (h) Guan, B. T.; Wang, Y.; Li, B. J.; Yu, D. G.; Shi, Z. J. *J. Am. Chem. Soc.* **2008**, *130*, 14468; (i) Gooßen, L. J.; Gooßen, K.; Stanciu, C. *Angew. Chem. Int. Ed.* **2009**, *48*, 3569; (j) Shimasaki, T.; Konno, Y.; Tobisu, M.; Chatani, N. *Org. Lett.* **2009**, *11*, 4890; (k) Kuroda, J.-i.; Inamoto, K.; Hiroya, K.; Doi, T. *Eur. J. Org. Chem.* **2009**, *2009*, 2251; (l) Zhao, Y. L.; Li, Y.; Li, Y.; Gao, L. X.; Han, F. S. *Chem. Eur. J.* **2010**, *16*, 4991; (m) Fan, X.-H.; Yang, L.-M. *Eur. J. Org. Chem.* **2010**, *2010*, 2457; (n) Yu, D.-G.; Li, B.-J.; Shi, Z.-J. *Acc. Chem. Res.* **2010**, *43*, 1486; (o) Chen, G.-J.; Huang, J.; Gao, L.-X.; Han, F.-S. *Chem. Eur. J.* **2011**, *17*, 4038; (p) Chen, H.; Huang, Z.; Hu, X.; Tang, G.; Xu, P.; Zhao, Y.; Cheng, C.-H. *J. Org. Chem.* **2011**, *76*, 2338; (q) Fan, X.-H.; Yang, L.-M. *Eur. J. Org. Chem.* **2011**, *2011*, 1467; (r) Xing, C.-H.; Lee, J.-R.; Tang, Z.-Y.; Zheng, J. R.; Hu, Q.-S. *Adv. Synth. Catal.* **2011**, *353*, 2051; (s) Gao, H.; Li, Y.; Zhou, Y.-G.; Han, F.-S.; Lin, Y.-J. *Adv. Synth. Catal.* **2011**, *353*, 309; (t) Mesganaw, T.; Garg, N. K. *Org. Process Res. Dev.* **2012**, *17*, 29; (u) Leowanawat, P.; Zhang, N.; Percec, V. *J. Org. Chem.* **2012**, *77*, 1018; (v) Li, X.-J.; Zhang, J.-L.; Geng, Y.; Jin, Z. *J. Org. Chem.* **2013**, *78*, 5078; (w) Hanley, P. S.; Ober, M. S.; Krasovskiy, A. L.; Whiteker, G. T.; Kruper, W. J. *ACS Catal.* **2015**, *5*, 5041; (x) Iranpoor, N.; Panahi, F.; Jamedi, F. *J. Organomet. Chem.* **2015**, *781*, 6; (y) Cornella, J.; Zarate, C.; Martin, R. *Chem. Soc. Rev.* **2014**, *43*, 8081.
10. (a) Quasdorf, K. W.; Riener, M.; Petrova, K. V.; Garg, N. K. *J. Am. Chem. Soc.* **2009**, *131*, 17748; (b) Antoft-Finch, A.; Blackburn, T.; Snieckus, V. *J. Am. Chem. Soc.* **2009**, *131*, 17750; (c) Quasdorf, K. W.; Antoft-Finch, A.; Liu, P.; Silberstein, A. L.; Komaromi, A.; Blackburn, T.; Ramgren, S. D.; Houk, K. N.; Snieckus, V.; Garg, N. K. *J. Am. Chem. Soc.* **2011**, *133*, 6352; (d) Leowanawat, P.; Zhang, N.; Resmerita, A. M.; Rosen, B. M.; Percec, V. *J. Org. Chem.* **2011**, *76*, 9946; (e) Zhang, N.; Hoffman, D. J.; Gutsche, N.; Gupta, J.; Percec, V. *J. Org. Chem.* **2012**, *77*, 5956; (f) Chen, G. J.; Han, F. S. *Eur. J. Org. Chem.* **2012**, 3575; (g) Leowanawat, P.; Zhang, N.; Safi, M.; Hoffman, D. J.; Fryberger, M. C.; George, A.; Percec, V. *J. Org. Chem.* **2012**, *77*, 2885; (h) Harris, M. R.; Hanna, L. E.; Greene, M. A.; Moore, C. E.; Jarvo, E. R. *J. Am. Chem. Soc.* **2013**, *135*, 3303; (i) Ramgren, S. D.; Hie, L.; Ye, Y.; Garg, N. K. *Org. Lett.* **2013**, *15*, 3950; (j) Jezorek, R. L.; Zhang, N.; Leowanawat, P.; Bunner, M. H.; Gutsche, N.; Pesti, A. K. R.; Olsen, J. T.; Percec, V. *Org. Lett.* **2014**, *16*, 6326; (k) Ke, H.; Chen, X.; Zou, G. *J. Org. Chem.* **2014**, *79*, 7132; (l) Malineni, J.; Jezorek, R. L.; Zhang, N.; Percec, V. *Synthesis* **2016**, *48*, 2808.
11. (a) Snieckus, V. *Chem. Rev.* **1990**, *90*, 879; (b) Board, J.; Cosman, J. L.; Rantanen, T.; Singh, S. P.; Snieckus, V. *Platinum Metals Rev.* **2013**, *57*, 234.
12. (a) García-Melchor, M.; Braga, A. A.; Lledós, A.; Ujaque, G.; Maseras, F. *Acc. Chem. Res.* **2013**, *46*, 2626; (b) Sperger, T.; Sanhueza, I. A.; Kalvet, I.; Schoenebeck, F. *Chem. Rev.* **2015**, *115*, 9532.
13. Zhang, K.; Conda-Sheridan, M.; Cooke, S. R.; Louie, J. *Organometallics* **2011**, *30*, 2546.
14. (a) Morrell, D. G.; Kochi, J. K. *J. Am. Chem. Soc.* **1975**, *97*, 7262; (b) Tsou, T. T.; Kochi, J. K. *J. Am. Chem. Soc.* **1979**, *101*, 7547; (c) Bakac, A.; Espenson, J. H. *J. Am. Chem. Soc.* **1986**, *108*, 719; (d) Anderson, T. J.; Jones, G. D.; Vicic, D. A. *J. Am. Chem. Soc.* **2004**, *126*, 8100; (e) Jones, G. D.; McFarland, C.; Anderson, T. J.; Vicic, D. A. *Chem. Commun.* **2005**, 4211; (f) Jones, G. D.; Martin, J. L.; McFarland, C.; Allen, O. R.; Hall, R. E.; Haley, A.

D.; Brandon, R. J.; Konovalova, T.; Desrochers, P. J.; Pulay, P.; Vicic, D. A. *J. Am. Chem. Soc.* **2006**, *128*, 13175; (g) Zhang, C.-P.; Wang, H.; Klein, A.; Biewer, C.; Stirnat, K.; Yamaguchi, Y.; Xu, L.; Gomez-Benitez, V.; Vicic, D. A. *J. Am. Chem. Soc.* **2013**, *135*, 8141; (h) Powell, D. A.; Maki, T.; Fu, G. C. *J. Am. Chem. Soc.* **2005**, *127*, 510; (i) Fischer, C.; Fu, G. C. *J. Am. Chem. Soc.* **2005**, *127*, 4594; (j) Dudnik, A. S.; Fu, G. C. *J. Am. Chem. Soc.* **2012**, *134*, 10693; (k) Schley, N. D.; Fu, G. C. *J. Am. Chem. Soc.* **2014**, *136*, 16588; (l) Phapale, V. B.; Bunuel, E.; Garcia-Iglesias, M.; Cardenas, D. J. *Angew. Chem. Int. Ed.* **2007**, *46*, 8790; (m) Cornella, J.; Gómez-Bengoa, E.; Martin, R. *J. Am. Chem. Soc.* **2013**, *135*, 1997; (n) León, T.; Correa, A.; Martin, R. *J. Am. Chem. Soc.* **2013**, *135*, 1221; (o) Breitenfeld, J.; Wodrich, M. D.; Hu, X. *Organometallics* **2014**, *33*, 5708; (p) Zheng, B.; Tang, F.; Luo, J.; Schultz, J. W.; Rath, N. P.; Mirica, L. M. *J. Am. Chem. Soc.* **2014**, *136*, 6499; (q) Lipschutz, M. I.; Tilley, T. D. *Angew. Chem. Int. Ed.* **2014**, *53*, 7290.

15. Guard, L. M.; Mohadjer Beromi, M.; Brudvig, G. W.; Hazari, N.; Vinyard, D. J. *Angew. Chem. Int. Ed.* **2015**, *54*, 13352.

16. (a) Pilloni, G.; Toffoletti, A.; Bandoli, G.; Longato, B. *Inorg. Chem.* **2006**, *45*, 10321; (b) Ge, S.; Hartwig, J. F. *Angew. Chem. Int. Ed.* **2012**, *51*, 12837; (c) Jin, D.; Schmeier, T. J.; Williard, P. G.; Hazari, N.; Bernskoetter, W. H. *Organometallics* **2013**, *32*, 2152; (d) Standley, E. A.; Smith, S. J.; Muller, P.; Jamison, T. F. *Organometallics* **2014**, *33*, 2012; (e) Wu, J.; Hazari, N.; Incarvito, C. D. *Organometallics* **2011**, *30*, 3142.

17. Sriram, D. *Medicinal Chemistry*; 2nd Ed. ; Pearson: New Delhi, 2010.

18. (a) Grushin, V. V.; Alper, H. *Chem. Rev.* **1994**, *94*, 1047; (b) Littke, A. F.; Dai, C.; Fu, G. C. *J. Am. Chem. Soc.* **2000**, *122*, 4020; (c) Parker, T. M., S. *Synthetic Methods in Organic Electronic and Photonic Materials: A Practical Guide*; Royal Society of Chemistry: Cambridge, 2015.

19. Partyka, D. V. *Chem. Rev.* **2011**, *111*, 1529.

20. The complex $^{\mathbf{dppf}}\mathbf{Ni}^{\mathbf{II(o\text{-}tol)(Cl)}}$ is commerically available from Aspira Scientific (www.aspirasci.com) with compound number 300926.

21. Beck, R.; Shoshani, M.; Krasinkiewicz, J.; Hatnean, J. A.; Johnson, S. A. *Dalton Trans.* **2013**, *42*, 1461.

22. Yin, G.; Kalvet, I.; Englert, U.; Schoenebeck, F. *J. Am. Chem. Soc.* **2015**, *137*, 4164.

23. (a) Heimbach, P. *Angew. Chem. Int. Ed.* **1964**, *3*, 648; (b) Tsou, T. T.; Kochi, J. K. *J. Am. Chem. Soc.* **1979**, *101*, 6319; (c) Uhlig, E.; Poppitz, W. *Z. Anorg. Allg. Chem.* **1981**, *477*, 167; (d) Kraikivskii, P. B.; Frey, M.; Bennour, H. A.; Gembus, A.; Hauptmann, R.; Svoboda, I.; Fuess, H.; Saraev, V. V.; Klein, H.-F. *J. Organomet. Chem.* **2009**, *694*, 1869; (e) Beck, R.; Johnson, S. A. *Organometallics* **2013**, *32*, 2944.

24. Hatnean, J. A.; Shoshani, M.; Johnson, S. A. *Inorg. Chim. Acta* **2014**, *422*, 86.

25. (a) Chatt, J.; Shaw, B. L. *J. Chem. Soc.* **1960**, 1718; (b) Hidai, M.; Kashiwag, T.; Ikeuchi, T.; Uchida, Y. *J. Organomet. Chem.* **1971**, *30*, 279; (c) Miyazaki, S.; Koga, Y.; Matsumoto, T.; Matsubara, K. *Chem. Commun.* **2010**, *46*, 1932; (d) Ge, S.; Green, R. A.; Hartwig, J. F. *J. Am. Chem. Soc.* **2014**, *136*, 1617; (e) Xu, H.; Diccianni, J. B.; Katigbak, J.; Hu, C.; Zhang, Y.; Diao, T. *J. Am. Chem. Soc.* **2016**, *138*, 4779.

26. The organic product 1-(2'-methylphenyl)naphthalene was also detected by GC. This is likely formed via disproportionation of $^{\mathbf{dppf}}\mathbf{Ni}^{\mathbf{Io\text{-}tol}}$ and $^{\mathbf{dppf}}\mathbf{Ni}^{\mathbf{Inap}}$ to generate $^{\mathbf{dppf}}\mathbf{Ni}^{\mathbf{II(o\text{-}tol)(nap)}}$ followed by reductive elimination; see the SI.

27. Standley, E. A.; Jamison, T. F. *J. Am. Chem. Soc.* **2013**, *135*, 1585.

28. For a review on the difficulties associated with modeling transmetallation in cross-coupling reactions using Pd catalysts see: Lennox, A. J. J.; Lloyd-Jones, G. C. *Angew. Chem. Int. Ed.* **2013**, *52*, 7362.

29. For examples of computational studies using the full base in transmetallation reactions using Ni complexes see: (a) Liu, L.; Zhang, S.; Chen, H.; Lv, Y.; Zhu, J.; Zhao, Y. *Chem. Asian J.* **2013**, *8*, 2592; (b) Muto, K.; Yamaguchi, J.; Musaev, D. G.; Itami, K. *Nat. Commun.* **2015**, *6*, 7508.

30. Benzene was used instead of toluene as the solvent for computational simplicity, as some reactions required the use of explicit solvent. For further details refer to the SI.

31. The DZP basis sets used with the M06L functional include the relativistic-ECP LANL2DZ(f) for Ni, 6-31+G(d) for Cl and 6-31G(d,p) for P, C, K and H. This theory level was used for full geometry optimization, without any geometry or symmetry constraints. Analytical frequencies were also computed with this DFT method to classify all stationary points as either minima (no imaginary frequencies) or transition states (single imaginary frequency). These calculations were used to determine the thermochemistry, including the zero-point, thermal and entropy energies for a 1M standard state. The potential energies were further refined with the M06 functional and the TZP basis sets, including the relativistic-ECP LANL2TZ(f) for Ni, 6-311+G(d) for Cl and 6-311G(d,p) for P, C, K and H. Further details on the computational methods are provided in the SI.

32. Based on a recent report (see Matsubara, K.; Yamamoto, H.; Miyazaki, S.; Inatomi, T.; Nonaka, K.; Koga, Y.; Yamada, Y.; Veiros, L. F.; Kirchner, K. *Organometallics* **2016**, In Press) we also modelled $^{\mathbf{dppf}}\mathbf{Ni}^{\mathbf{Isulf}}$ as a dimeric species. The formation of the dimeric species is endoergic from the monomer by 2.6 kcal mol^{-1}.

33. Zheng, W.; Ding, L.; Wang, J.; Wang, Y. *RSC Adv*. **2016**, *6*, 26514.

TOC Graphic

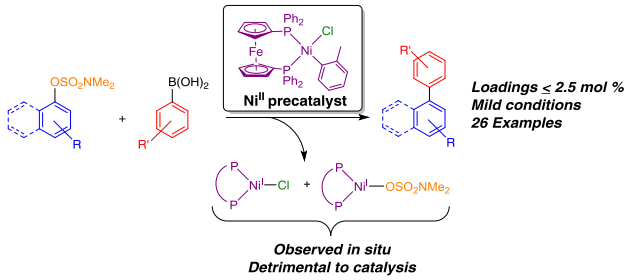
OSO2NMe2
B(OH)2
R
R'
Ni^II precatalyst
Loadings ≤ 2.5 mol %
Mild conditions
26 Examples
Observed in situ
Detrimental to catalysis